Fundamental Investigation of Saturated Flow Through Porous Media with Macropores

by

Yumao Jin

A thesis submitted to the Graduate Faculty of
Auburn University
in partial fulfillment of the
requirements for the Degree of
Master of Science

Auburn, Alabama
May 7, 2012

Keywords: Macropore, Hydraulic Conductivity

Approved by

Dr. Navin Kumar C. Twarakavi, Chair, Assistant Professor of Agronomy and Soils
Dr. T. Prabhakar Clement, Professor and Arthur H. Feagin Chair of Civil Engineering
Dr. Joey Shaw, Professor of Agronomy and Soils
Dr. Francisco J. Arriaga, Affiliate Associate Professor of Agronomy and Soils

Abstract

Among the foremost issues in the area of hydrological sciences is the estimation of infiltration fluxes and the associated contaminant exchange from the near-surface to the ground water table. While the simplest and traditional conceptualization of infiltration is that of a uniform, downward-advancing wetting front in a homogeneous medium, field observations indicate that it is highly nonuniform. Macropores are ubiquitously found in the subsurface and have a significant impact on hydrological processes. The presence of macropores leads to preferential water flow through both unsaturated and saturated soils, which are difficult to predict. In the first part, the effect of macropore density and connectivity on water flow in porous media was studied by comparing the hydraulic conductivity of different distributions of artificial macropores. The effective hydraulic conductivity was measured by constant head method, and the artificial macropores are prepared with stainless steel mesh reinforcements used in co-axial cables. The result shows that as macropores become increasingly discontinuous, the hydraulic conductivity approaches the value of no-macropore media. Also, the extent of effects of macropore connectivity on the hydraulic conductivity decreases with coarser media. Since the velocity in macropores could be large in certain cases, we have also investigated the validity of Darcy's Law under high Reynolds number conditions. Ergun equation is one of the most common empirical formulations that used to model porous media flow in high Reynolds number systems. In this study, we have formulated

a new form of Ergun equation, identified as the inverted Ergun (IE) equation, which is more appropriate for modeling hydrological problems. The validity of the IE equation has been tested by using various forms of error analyses and also by using experimental datasets. The results show that IE equation is a useful alternative for modeling high velocity flows in porous media systems.

Acknowledgments

I would like to sincerely thank my advisor, Dr. Navin Kumar C. Twarakavi. His continuous support, encouragement and valuable suggestions played a vital role in the achievement of this research. I would like to extend my thanks to my advisory committee members: Dr. Prabhakar Clement, Dr. Joey Shaw and Dr. Francisco Arriaga for their participation in my thesis committee. I would also like to thank Dr. Laurent Bahaminyakamwe for his support and help in setting up my experiments.

I take immense pleasure in thanking my family members for believing in me and standing beside me at every step till today. Special thanks to Gerald, Robert and fellow graduate students for their aid, support and friendship. Finally, I would like to thank all my friends for their unwavering support and timely help.

Table of Contents

List of Tables

List of Figures

List of Abbreviations

ADE	Advection Dispersion Equation
ARS	Agriculture Research Service
CDE	Convection–Dispersion Equation
REV	Representative Elementary Volume
Eqn	Equation
Ksat	Saturated Hydraulic conductivity

I. Literature Review

Introduction

Macropores are large, continuous voids in soil and include structural, shrink-swell, and tillage fractures, old root channels, and soil fauna burrows (Radcliffe D. E. 2008). The macropores in soils are very important in controlling the movement of water under both saturated and unsaturated conditions. Beven and Germann (1981) noted that water will move through large voids under saturated conditions, and that they may greatly influence the saturated hydraulic conductivity of soils, even though they may contribute only a very small amount to the total porosity of a soil. For unsaturated soil, the presence of macropores leads to variation in water flow that is not described well by a Darcy approach to flow through porous media. Macropores are readily visible and are often continuous for distances of at least several meters in both vertical and lateral directions.

There are standard definitions and classfications of macropore based on pore size. Luxmoore (1981) suggested that the equivalent pore diameter range of macropore is longer than 1000 μm. Beven and Germann (1981) considered that only the pores greater than 3000 μm in diameter can be defined as macropores. However, Marshall (1959) estimated the equivalent diameter of a macropore is above 30 μm. Luxmoore (1981) conducted a literature review and noted that non-capillary porosity has also been used to distinguish large pores from small pores. Nelson and Baver (1940) estimated non-capillary porosity for several materials as the pore volume that became water filled above approximately -3 Pa pressure. Marshall (1959) expressed an updated viewpoint that equated non-capillary porosity with macroporosity. They define macroporosity as the pore volume that becomes water filled at pressures above -10 kPa.

However, Ranken (1984) suggested it should be above -1.0 kPa, and Bullock and Thomasson (1979) believed it should be above -5.9 kPa.

Brewer (1964) proposed the following pore equivalent diameter (μm) classes: coarse macropores, > 5000 μm; medium macropores, 2000 μm to 5000 μm; fine macroproes, 1000 μm to 5000 μm; very fine macropores, 75 μm to 1000 μm. Reeves (1980) developed a different classification: enlarged macro-fissures of equivalent diameter should be in the range of 1000 μm to 20000 μm; macro-fissures should be in the range of 200 μm to 2000 μm. Russell (1973) adopted a somewhat different classification, the diameter of coarse macropores should be greater than 200 μm; medium, 20 μm to 200 μm; fine, 2 μm to 20 μm; and very fine < 2 μm. However, Bouma et al (1989a) pointed out that size is less important than pore continuity; small pores with a diameter of 40 μm can conduct considerable quantities of water if they are continuous throughout a soil sample, which implies that the conductivity also plays an important role in the definition of macropores.

Macropore type and physical characteristics

Beven and Germann (1981) suggested that on the basis of morphology, macropores may be grouped as the following:

1. Biopores: Pores formed by the soil fauna and soil flora. They are primarily tubular in shape, but the size may extend from less than 1 mm to over 50 mm in diameter. Biopores are concentrated close to the soil surface. Perret et al. (1999) investigated the geometry of macropore networks consisting of cylindrical biopores larger than 1 mm in diameter in an uncultivated sandy loam soil under grass. They identified more than 13000 such branching networks per m^3 of soil, which corresponds to a total macroporosity of between 2% to 4%. The networks had a geometric mean volume of 50 mm^3 and a tortuosity between 1.2 and 1.3, and

their modal length was 40 mm (cited by Jarvis 2007). Shipitalo and Butt (1999) reported that the tortuosity of channels produced by deep-burrowing earthworms is 1.1 to 1.2. In contrast, since endogeic earthworm species feed and burrow only within the topsoil, they produce temporary burrows that are more randomly oriented, shorter, more tortuous, and branched (Capowiez et al., 2001; Je ́gou et al., 2001), and which therefore may have more limited effects on water flow and solute transport (Ela et al., 1991).

Biopores are also commonly formed by plant roots, which also constitute important pathways for non-equilibrium flow and transport. For example, Tippkotter (1983) reported interconnected networks of tubular pores 0.1–0.6 mm in diameter, with a similar morphology to that of living root systems at more than 1-m depth in a loess soil. Edwards et al. (1988) counted more than 14,000 cylindrical macropores larger than 0.4 mm in diameter per m^2 in an untilled silt loam soil cropped with maize. Of these, 80% were less than 1-mm in diameter and were presumed to be channels created by decayed roots.

2. Pores created by cracks and fissure. These macropors are formed either by shrinkage resulting from dessication of clay soils (e.g.,Blake et al., 1973; Lewis, 1977) or by chemical weathering of bedrock materials (e.g., Reeves, 1980). Chertkov and Ravina (1999) reported that the tortuosity of crack networks in clayey soils ranged from 1.2 to 2.0.

3. Natural soil pipes. Natural soil pipes may form because of the erosive action of subsurface flows, where the forces imposed on individual soil particles caused by the flow exceed the structural competence of the soils (e.g., Zaslavsky and Kassif, 1965).

Chemical and Biological characteristics of macropores

Apart from physical characteristics such as size, continuity and surface area, the biological and chemical properties of macropores are very different to those of the bulk soil

(Jarvis, N.J. 2007). Roots are often preferentially close to macropores, and often in direct contact with the macropore wall, which means water and air do not have long distances to travel to the roots if they enter the soil through the macropores. Thus, macropores are close to the zone of maximum organic matter cycling, microbiological activity, and hence, nutrient availability (Stewart et al., 1999). Accelerated degradation of organic contaminants has been found in artificial macropores, which was attributed to favorable conditions for biofilm development, and improved aeration and supply of substrates (Pivetz & Steenhuis, 1995; Pivetz et al., 1996, cited by Jarvis). Bundt et al. (2001b) stained preferential flow paths in a forest soil with a food dye and sampled soil materials from preferential flow paths to evaluate microbial biomasses and microbial community structures. They found that the preferential flow paths are more exposed to drying and wetting than the soil matrix, which allows better nutrient and substrate supply than the soil matrix. Favorable living conditions in preferential flow paths are reflected by significantly larger microbial biomasses.

Water flow in Macropores

Lawes et al. (1882) noted that *"... in a heavy soil, channel drainage will in most cases precede general drainage, a portion of the water escaping by the open channels before the body of the soil has become saturated; this will especially be the case if the rain fell rapidly, and water accumulates on the surface".* Hendrickx and Flury (2001) defined preferential flow as "all phenomena where water and solutes move along certain pathways, while bypassing a fraction of the porous matrix". Bouma (1981) mentioned that preferential flow in saturated soil involves rapid displacement of water from macropores (hydrohynamic dispersion). In unsaturated soil, flow into air-filled macropores (short-circuiting) occurs, which is followed by lateral absorption.

Since there are a number of different causes of preferential flow, each process has a separate term. For instance, macropore flow is used to indicate preferential flow in continuous root channels, earthworm burrows, fissures, or cracks within well-structured and mostly fine-textured soils. Flow paths can vary in type from individual pores to a highly connected pore network and pore geometries that range from cylindrical to slabs, and dimensions may vary from capillary size to larger (Gerke. H.H 2006). Under both saturated and unsaturated conditions, water can move downslope through macropores very rapidly (of the order of a meter per hour, Beven & Germann, 1982). Mosley (1982) recorded mean macropore flow velocities ranged from 0 to 0.0098 ms^{-1}. Newson and Harrison (1978) conducted tracer experiment in a natural pipe, and found that macropore flow mean velocity ranged from 0.06 to 0.2 ms^{-1}.

Beven and Germann (1982) noted that macropore flow results when vertical flow rates in macropores are more rapid than the lateral equilibration of matrix water pressure.. Classical theory of water flow (Richards' equation) and solute transport (ADE) is based on the assumption that unique values of soil water pressure and solute concentration can be defined for a representative elementary volume (REV). Physical non-equilibrium occurs in the soil unsaturated zone when heterogeneities result in the generation of lateral differences (non-uniformity) either in water pressures or solute concentrations, or both, during vertical flow and transport, which invalidates the REV concept (Jarvis, N. J 2007).

Jarvis (2007) discussed the causes and consequences of 'non-equilibrium' water flow and solute transport in large structural pores or macropores, He pointed out that macropore size, continuity and the presence of impermeable linings and coatings that restrict lateral mass exchange were able to initiate rapid non-equilibrium flow. Jarvis also explained that water flow

in soil pores is driven by gravity, capillarity, viscous forces and inertial forces; the same forces that operate on all pores in soil no matter their sizes, so in this respect macropore flow does not differ from matrix flow. However, when gravity dominates the driving force, the velocities in macropores may become very large, and the acceleration term in momentum balance may not always be negligible, an assumption which is implicit in the derivation of Darcy's law and the Richards' equation. This can be illustrated by calculating the Reynolds number as a function of pore diameter, assuming fully saturated laminar flow in straight-sided cylindrical macropores in accordance with Hagen–Poiseuille's law. The Reynolds number (a dimensionless parameter) for porous media flow is typically expressed as [1.1].

$$Re=(\rho v d_{30})/\mu$$

where ρ is the density of water (units of mass per volume), v is the specific discharge (not the pore velocity — with units of length per time), d_{30} is a representative grain diameter for the porous media (often taken as the 30% passing size from a grain size analysis using sieves with units of length), and μ is the fluid viscosity (Todd, 1959).

The Reynolds number, which is a measure of the ratio of inertial to viscous forces, exceeds unity and therefore invalidates Darcy's law (Childs, 1969) at pore diameters larger than 0.15 mm. Darcy's law is only valid for slow, viscous flow; apparently, most groundwater flow falls in this category. Typically, any flow with a Reynolds number less than one is clearly laminar, and it would be valid to apply Darcy's law. Furthermore, experimental tests have shown that flow regimes with Reynolds numbers up to 10 may still be Darcian.

Logsdon (1993) determined that the Reynolds numbers were larger than 1000 for flow through a partially saturated artificial macropore 6-mm in diameter open to a supply of free water at the soil surface. Mori et al. (1999a, cited by Jarvis N. J. 2007) reported Reynolds

numbers varied between 50 and 80 for flow in natural soil macropores under ponded infiltration, which suggested that the flow regime could be transitional to turbulent.

Jarvis (2007) explained non-uniform flow during infiltration by using a soil block containing macropores. In the initial dry state (point A, See Figure 1.1), the matrix hydraulic conductivity dominates the flow, and the macropore hydraulic conductivity is negligible. The water entry pressure of smaller macropores is reached at pressure potential B and non-equilibrium begins to develop, but the additional contribution of these pores is not dramatic. The pressure potential, at C, is only slightly larger than at B or A, but the hydraulic conductivity is orders of magnitude larger since large vertically continuous macropores begin to conduct water. The soil now wets up in a markedly non-uniform manner with water flowing rapidly in macropores, far ahead of the matrix wetting front.

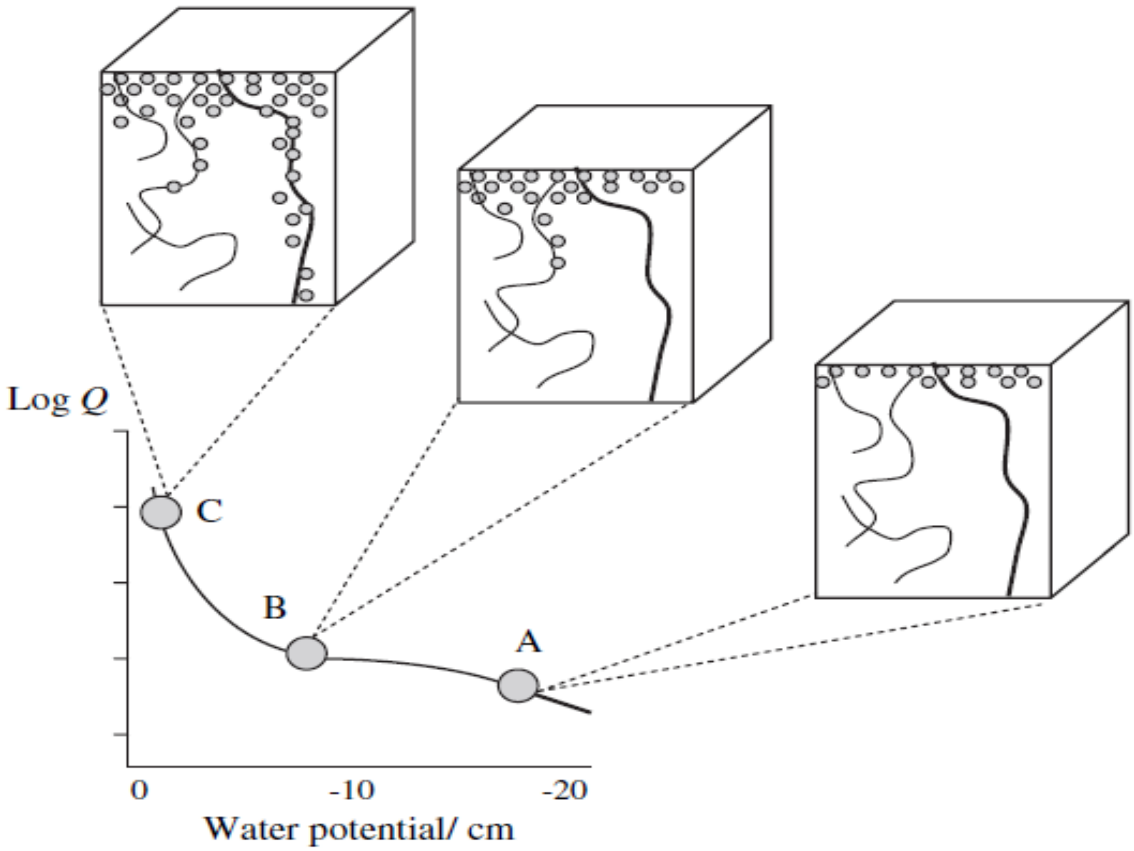

Figure 1.1. Schematic diagram illustrating the water potential attained at the soil surface under different infiltration rates, Q, and the generation of non-equilibrium flow in macropores (Jarvis N. J. 2007).

Dynamics of Macropores

Changes in the soil-plant-animal community and in external conditions, such as the pattern of weather, will affect the balance between constructive and destructive processes (Beven and Germann 1982). Moreover, longer-term climatic changes, long-term ecological changes and land use affect the macropore system through its effect on the soil-plant-animal community. Land use plays an important role in the development of macroporosity. For instance, the number of earthworm channels in the surface layer of a tilled soil is much less than in a comparable untilled area (Ehlers,W., 1975). Soil macroporosity and the proportion of rainfall moving through preferential flow paths often increases with the adoption of conservation tillage, which contributes to a reduction in surface runoff (Shipitalo et al., 2000).

Green and Askew (1965) reported that macropores created by ants may last several hundreds of years. Beven and Germann (1982) reported that macropores formed from tree roots may last at least 50-100 years in a soil containing about 30% clay. The effective lifetime of macropores may be assumed to increase with stability of the soil structure, which is in itself a function of soil texture, mineralogy, and the composition of organic matter.

Studies of macropores

Beven and Germann (1982) mentioned that there are two types of large voids in soil: voids that are hydrologically effective in terms of channeling flow (macropores), and those that are not. Any experimental technique used to determine soil macroporosity should differentiate them.

Jarvis (2007) suggested that soil and crop management practices strongly modify soil structure and therefore affect the extent of non-equilibrium flow and transport in macropores. Edwards et al. (1992) compared water flows measured from large diameter earthworm burrows

(*Lumbricus terrestris L.*) in paired fields under no-till maize and grassland, and found that 60% less macropore flow occurred at the grassland site during one growing season. Booltink and Bouma (1981) conducted an experiment in two large undisturbed soil monoliths using breakthrough curves, and noted that large and well-connected macropores are able to transmit water and tracer more rapidly than small, tortuous, and less well-connected macropores.

Macropore flow has a significant influence on the leaching of agrochemicals. Shipitalo et al (2000) reported that if a heavy, intense storm occurs shortly after surface application of an agricultural chemical to soils with well-developed macroporosity, the water transmitted to the subsoil by the macropores may contain significant amounts of applied chemical, regardless of the affinity of the chemical for the soil. This amount can be reduced by an order of magnitude or more with the passage of time, or if lighter intensity precipitation precedes the first major leaching event. They explained that solutes normally strongly adsorbed by the soil are subject to leaching in macropores in the first few storms after application. Jarvis (2007) mentioned that the impact of macropore flow on leaching depends strongly on the properties of the chemical under consideration, particularly its sorption characteristics, the nature of any biological transformations, and whether the solute is surface-applied or indigenous to the soil (White, 1985a; Elliott & Coleman, 1988; Jarvis, 1998).

FOCUS (2001) reported that macropore flow effects on pesticide leaching are typically less than 1% of the applied dose, but losses of between 1 and 5% can occur. In some hydrogeological formations, such as clayey glacial tills, or fractured chalk and limestone, non-equilibrium transport in fissures can be continuous to great depth, and can be a dominant mechanism for pesticide transport towards important underlying drinking water aquifers (Jørgensen et al., 1998; Haria et al., 2003; Stenemo et al., 2005; Roulier et al., 2006). However,

Jarvis (2007) noticed that in many loamy and clayey soils prone to macropore flow, the deeper subsoil below the rooting depth is much less permeable due to the absence of structure-forming processes, so that most excess water is routed to surface water via field drainage systems rather than to groundwater.

The occurrence of macropore flow dramatically increases the leaching of otherwise "non-leachable" (i.e. strongly sorbed or fast degrading) compounds, although it will have less effect on highly mobile or persistent compounds (Larsson & Jarvis, 2000). In field experiments, leaching losses of phosphorus in macropore flow to subsurface drainage systems have been reported to range from 0.2 to 5 kg $ha^{-1}year^{-1}$ in loamy and clayey soils, with particle bound transport accounting for 10 to 75% of the total (e.g. Heckrath et al., 1995; Ule ń & Persson, 1999; Hooda et al., 1999; Addiscott et al., 2000). Priebe and Blackmer (1989) conducted an experiment to evaluate the possibility that preferential movement of water through soil macropores was an important factor in losses of surface-applied urea and nitrate from Iowa soils. Their studies showed that large nitrate losses occur due to macropore flow following fertilizer application. Camobreco et al. (1996) demonstrated that preferential flow plays a crucial role in transporting metals through a soil profile, as illustrated by the fact that the homogenized matrix flow columns adsorbed all applied metals while the undisturbed preferential flow columns allowed some of the metals to pass. Gjettermann et al. (2004) conducted an experiment to investigate the effect of macropore flow (i.e., film and pulse flow) on the interaction of solutes with macropore walls. They studied orthophosphate (P) transport and sorption in artificial macropores, and found that P concentration in macropores decrease much more during film flow than during pulse flow.

Macropore Modeling

Gerke (2006) mentioned that in heterogeneous structured soils, water, dissolved substances, suspended particles, and colloids may under certain conditions bypass most of the soil porous matrix thereby creating non-equilirium conditions in pressure heads, and solute concentration gradients between preferential flow paths and the soil matrix. The discussion of modeling of macropores is actually the study of preferential flows, which severely limits the applicability of standard models for flow and transport that are mostly based on the Richards' equation and the convection-dispersion equation (CDE). Beven (1991) reported that during wetting, part of the moisture front can propagate quickly to significant depths, and water and solutes may move to far greater depths much faster than predicted with the Richards' equation using area-averaged moisture contents and pressure heads. Another important characteristic of preferential (non-uniform) flow is its non-equilibrium nature. Even for uniform flow conditions, most of the water and its dissolved solutes generally move through the largest continuous pores that are filled with water at a particular tension. This is reflected in the shape of the highly non-linear hydraulic conductivity function, which typically shows dramatic increases with increasing water contents, particularly as the larger pores become conductive. While conditions at or close to equilibrium exist between the different types of pores in a soil during uniform flow, this is generally not the case during preferential flow (Šimůnek et al., 2003).

Preferential flow in structured media (both macroporous soils and fractured rocks) can be described using a variety of dual-porosity, dual-permeability, multi-porosity, and multi-permeability models. Dual-porosity and dual-permeability models assume that the porous medium consists of two interacting regions, one associated with the inter-aggregate, macropore, or fracture system, and one comprising micropores (or intra-aggregate pores) inside soil

aggregates or the rock matrix (Pruess and Wang, 1987; Gerke and van Genuchten, 1993a; Gwo et al., 1995; Jarvis, 1998, cited by Šimůnek et al., 2003).

Process-based models for flow and transport in granular (or single-porosity) media are generally based on the Richards' equation for variably saturated water flow and the convection–dispersion equation (CDE) for solute transport,

$$\frac{\partial\theta}{\partial t}=\frac{\partial}{\partial z}\left[K(\theta)\left(\frac{\partial\psi}{\partial z}+1\right)\right]$$

where K is the hydraulic conductivity, ψ is the pressure head, z is the elevation above a vertical datum, θ is the water content, and t is the time.

Gerke and Genuchten (1993) noted that a one-dimensional dual-porosity model has been developed for the purpose of studying variably saturated water flow and solute transport in structured soils or fractured rocks. This model involves two components at the macroscopic level: a macropore or fracture pore system and a less permeable matrix pore system. Central to the dual-porosity approach is the assumption that the medium can be separated into two distinct pore systems. Water flow in both the matrix and in fracture pore (macropore) is assumed to be mobile, and is described with the Richards' equation, and solute transport is described with the CDE (Gerke and Genuchten 1993). Dykhuizen (1987) postulated that the dual-porosity medium is a superposition of these two systems over the same volume. While dual-porosity models assume that water in the matrix is stagnant, dual-permeability models allow for water flow in the matrix as well.

Ahuja et al (1993) used the USDA-ARS Root Zone Water Quality Model to study macropore flow and transport in a silty clay loam soil, which is based on a two-domain (soil matrix and macropore) approach. They found that the macropore size had very little effect on

macropore flow and transport, but the smallest pores retarded the downward chemical movement by wall adsorption slightly more than the largest size pores.

Fluid Flow through Porous Medium

Henry Darcy connected the fountains of the city of Dijon in France with homogeneous sand filters in 1856. Darcy concluded that the rate of water flow Q (volume per unit time) is: (a) proportional to the constant cross-section area A of the sand filter, (b) proportional to hydraulic head (h_1-h_2) and (c) inversely proportional to the length L. When combined, these conclusions provide Darcy's Law:

$$Q=KA(h_1-h_2)/L$$

where the coefficient of proportionality K is called hydraulic conductivity, and (h_1-h_2) is the difference in hydraulic head across the filter of length L. As the hydraulic head defines (in terms of head of water) the sum of pressure and potential energies of the fluid per unit weight, (h_1-h_2)/L is interpreted as the hydraulic gradient. Denoting this gradient by J and defining the specific discharge, q, as discharge per unit cross-sectional area normal to the direction of flow ($q=Q/A$), we obtain:

$$q=KJ;\ J= (h_1-h_2) / L$$

Darcy's equation is analogous to the electrical and heat flow equations, in which the proportionality factors are termed "electrical conductivity" and "thermal conductivity", respectively.

Hydraulic conductivity (K) is a scalar (dimensions L/T) that expresses the ease with which a fluid is transported through a porous matrix. It is, therefore, a coefficient that depends on both matrix and fluid properties. The relevant fluid properties are density (ρ), and viscosity (μ), or, in the combined form, kinematic viscosity (ν). The relevant solid matrix properties are

mainly grain (or pore) size distribution, shape of grains (or pores), tortuosity, and specific surface. The hydraulic conductivity K was expressed by Nutting (1930) as:

$$K=kg/\nu$$

where k (dimension L^2)—called the permeability (or intrinsic permeability) of the porous matrix , and is restricted to properties of the medium alone (Bear, J. 1972).

The intrinsic permeability can be expressed as:

$$k=cd^2$$

where c is a dimensionless constant, usually including properties such as path tortuosity, particle shape, sediment sorting, and possible porosity; and d is either pore diameter or a representative grain diameter (Bear, 1972; Freeze and Cherry, 1979). However, Shepherd (1989) performed statistical power regression analysis on 19 sets of published data on size and laboratory permeability of unconsolidated sediments, and found that the exponent of grain diameter ranged from 1.11 to 2.05, and most values were significantly less than 2.0:

$$k=cd^{1.65\text{-}1.85}$$

where c is a dimensionless constant, usually held to include properties such as path tortuosity, particle shape, sediment sorting, and possible porosity; and d is either pore diameter or a representative grain diameter.

Determining the K of soils can be done with correlation or hydraulic methods. Hydraulic methods can be either laboratory methods or in-situ (or field) methods. The hydraulic methods are based on imposing certain flow conditions in the soil and applying an appropriate formula based on Darcy's Law and the flow boundary conditions. The K is calculated using the values of hydraulic head and discharge observed under the imposed conditions. The hydraulic laboratory methods are often applied to soil cores. Although these

methods are more laborious than correlation methods, they are still relatively fast and cheap, and they eliminate the uncertainty associated with relating soil properties to K (H.P.Ritzema, 1994).

II. Macropore Density and Connectivity Effects on Hydraulic Conductivity

Introduction

Macropore flow in soil has important consequences on ground water quantity and quality since water and pollutants can be transported through macropores rapidly. Water flow and solute movement through macropores can be affected by the density of the macropores, size of macropores, the presence of clay coatings, biological activity, the vertical flow rates, and the extent of 'direct connectivity' between the macropores and the surface (Javis 2007).

Macropores can be defined and classified according to their size. Luxmoore (1981) conducted a literature review and noted that non-capillary porosity has also been used to distinguish large pores form small pores, and suggested that if the diameter of pores are wider than 1000 μm, we can call them macropores. However, there are many other definitions of the macropore based on their size. For instance, Beven and Germann (1981) defined macropores as those pores with a diameter greater than 3000 μm. Marshall (1959) estimated the equivalent diameter of macropore to be above 30 μm. We can see that the definition of the macropore based on their sizes is not well defined. In a literature review, Jarvis (2007) discussed the causes and consequences of 'non-equilibrium' water flow and solute transport in large structural pores or macropores, and pointed out that the large size, continuity and presence of impermeable linings and coatings that restrict lateral mass exchange can cause rapid non-equilibrium flow in macropores. Jarvis (2007) also explained that water flow in soil pores is driven by gravity, capillarity, viscous forces and inertial forces, which are the same forces that operate in all soil pores no matter their size, thus in this respect macropore flow does not differ from matrix flow. However, when gravity dominates the driving force, the velocities in

macropores can become very large, and the acceleration term for the momentum balance may not always be negligible, an assumption for Darcy's law and Richards' equation.

What constitutes a macropore cannot be defined purely based on the size of the macropore. Instead, the dynamics of the flow in macroporous soils determines if the soil is "Macroporous". In other words, one needs to consider the macropore density and inter-macropore connectivity relative to the type of porous media before determining if the soil is macroporous. For example, an elaborate macropore network may have minimal effect on water flow and solute transport in a coarse sand as opposed to a single continuous macropore in a clayey soil. In order to better understand the definition of macropores, we use artificial macropore structures of different density and connectivities to study their effect on the effective hydraulic conductivity of the porous media. Note that one could also look at solute transport aspects to study macropore effects, which is a subject of future research. For the purposes of this research, we compare the effective hydraulic conductivity of the Macroporous porous media with that of the bulk matrix to draw conclusions on macropore effects on water flow.

Materials and Methods

Materials

Three different sizes of glass-beads, with diameters of 0.5mm (fine glass beads, FGB), 1.15mm (medium glass beads, MGB), 1.9mm (large glass beads, LGB) and two different Ottawa silica sands of average grain diameter 0.29 mm (No. 40-60 sand) and 1.1mm (No. 12-20 sand) were used. All the glass-beads and silica sand were washed repeatedly with 1.0 mol/L HCl, 1.0 mol/L NaOH and deionized water to ensure clean porous media for our experiments.

Dual-permeability models are commonly used to represent the flow in macroporous soils. In dual-permeability models, the flow in soils is conceptualized as two separate flow domains interacting with each other. The interaction is represented using a transfer coefficient. If dual-permeability models are to be used, one needs to incorporate values for the hydraulic conductivity of the matrix and the macropores. While the hydraulic conductivity of the bulk matrix can be estimated using traditional approaches, estimating the hydraulic conductivity of the macropores is not straight forward. We estimated the hydraulic conductivities of the macropore domain for different porous media under conditions of varying inter-macropore connectivity and densities using MODFLOW, which is the U.S. Geological Survey modular finite-difference flow model.

The glass-bead material formed the bulk matrix in to which macropore structures were added. Artificial macropores were made by using stainless steel mesh reinforcement used in co-axial cables (Figure 2.1). These stainless steel mesh reinforcements are good proxies for macropores because: (a) they have a fixed diameter throughout and are made of very porous walls with same sizes of pores. (b) the stainless steel mesh reinforcements allow for free movement of water through their walls and at the same time, resist collapse of the bulk matrix around it. The diameter of the artificial macropores used in our study was 0.3 mm. Through our experiments, we used deionized and degassed water in order to maintain saturated conditions during the setup and experimental process.

Figure 2.1 Artificial macropores were constructed from the braided metallic shielding material in coaxial wires.

.

Experiment Setup

We used a constant head to measure the saturated hydraulic conductivity of the porous matrix with macropores. In this experiment, a 2.64 cm diameter by 38.2 cm long glass column was used to measure the effective hydraulic conductivities of different porous matrices and macropore combination. Because the grains of the porous media are nearly spherical, the porosity of the column was assumed to be 0.4. The column was uniformly packed with porous media under wet conditions to ensure there was no air in the column. The schematic of the setup is shown in Figure 2.2. The saturated column was connected to a water tank, water was allowed to flow vertically from the bottom to top at a constant head of 3-cm of water. The volume of water that passed through the column over a period of time, t, was measured. Re-arranging Darcy's law and solving for K_s, we obtain eqn. [2.1]

$$K_s = \frac{VL}{At(H_2 - H_1)} \qquad \text{----------}$$

[2.1]

where K_s is the effective saturated hydraulic conductivity of the porous media, *V* is the volume of water that flows through the sample of cross-sectional area *A* during time *t* and $(H_2 - H_1)$ is the hydraulic head difference imposed across the sample of length *L*.

Experimental Procedure

The macroporosity (or macropore density) of a porous media can be calculated using following equations:

$$\text{Macroporosity} = \frac{V_{mac}}{Vmac+Vmic} \qquad \text{--------[2.2]}$$

$$V_{mic} = n*(V - V_{mac}) \qquad \text{--------[2.3]}$$

where V_{mac} refers to the volume of macropores, V_{mic} is the volume of the matrix without the macropore, *V* is the volume of the column and *n* is the porosity of the medium. We used reference value as 0.4 here. Macroporosity refers to the relative fraction of pores that can be classified as macropores in the porous media. For each porous media, the following macropore densities (or macroporosities) were considered: 2.97% (hereby, called D1) and 5.87% (hereby, called D2).

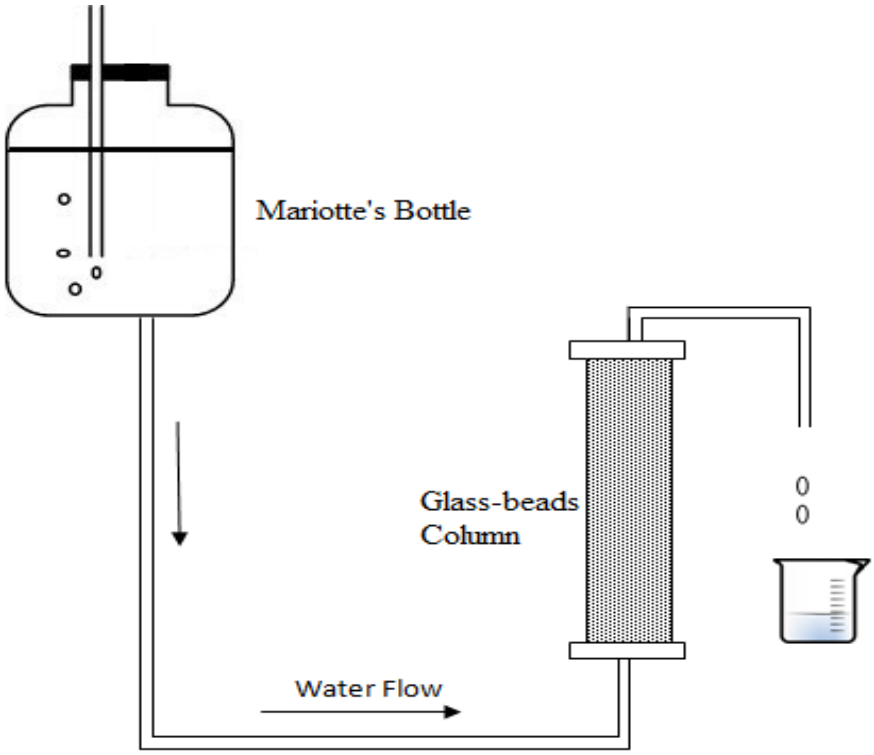

Figure 2.2. Schematic of the experimental setup to estimate hydraulic conductivity using constant head method. The column is connected to a Mariotte bottle filled with degassed de-ionized water.

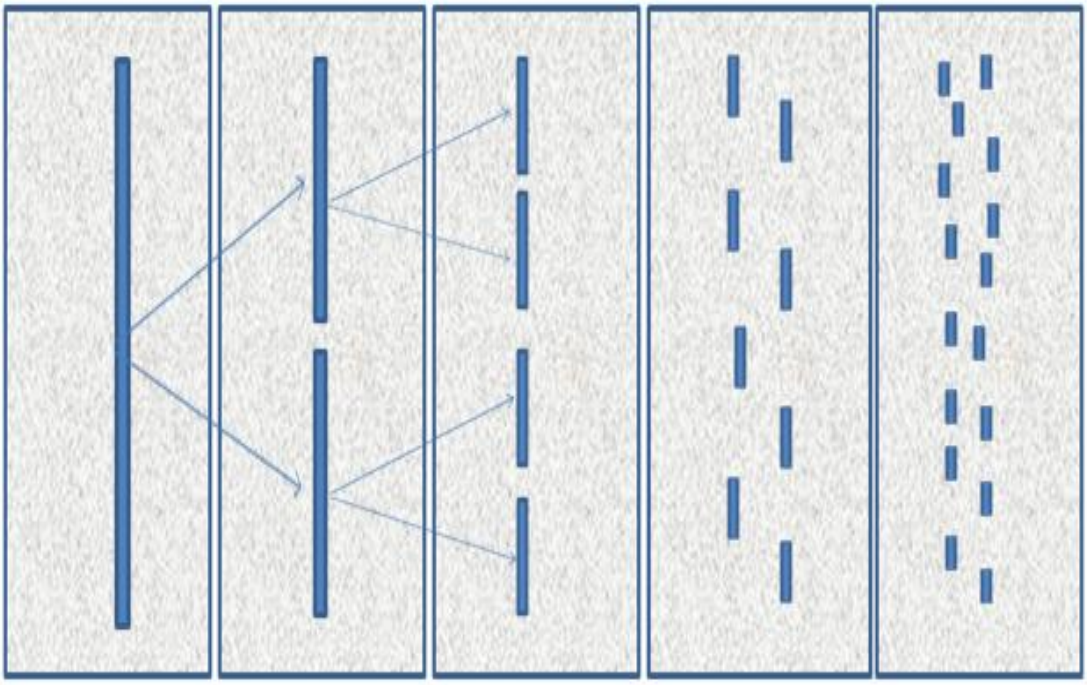

Figure 2.3. Schematic showing macropore distribution (connctivity) in the column for the 2.97% (D1) macropore system.

For macropore density of D1, we created different inter-macropore connectivities by allocating the macroporosity in to 1, 2, 4, 8 and 16 equally- sized artificial macropores (Figure 2.3). These inter-macropore connectivities are referred to as C1, C2, C3, C4 and C5, respectively. As the number of artificial macropores increased for a given macropore density, the macropores become more discontinuous.

Similarly, for a macropore density of 5.87% (D2), we created different inter-macropore connectivities by allocating the macroporosity in to 2, 4, 8, 16 and 32 equally- sized artificial macropores (Figure 2.4). Note that the macropore density of D2 (5.87%) is nearly double the macropore density of D1 (2.97%). Therefore, these inter-macropore connectivities are also referred as C1, C2, C3, C4 and C5 respectively because the lengths of each macropore for a given connectivity is same for both macropore densities.

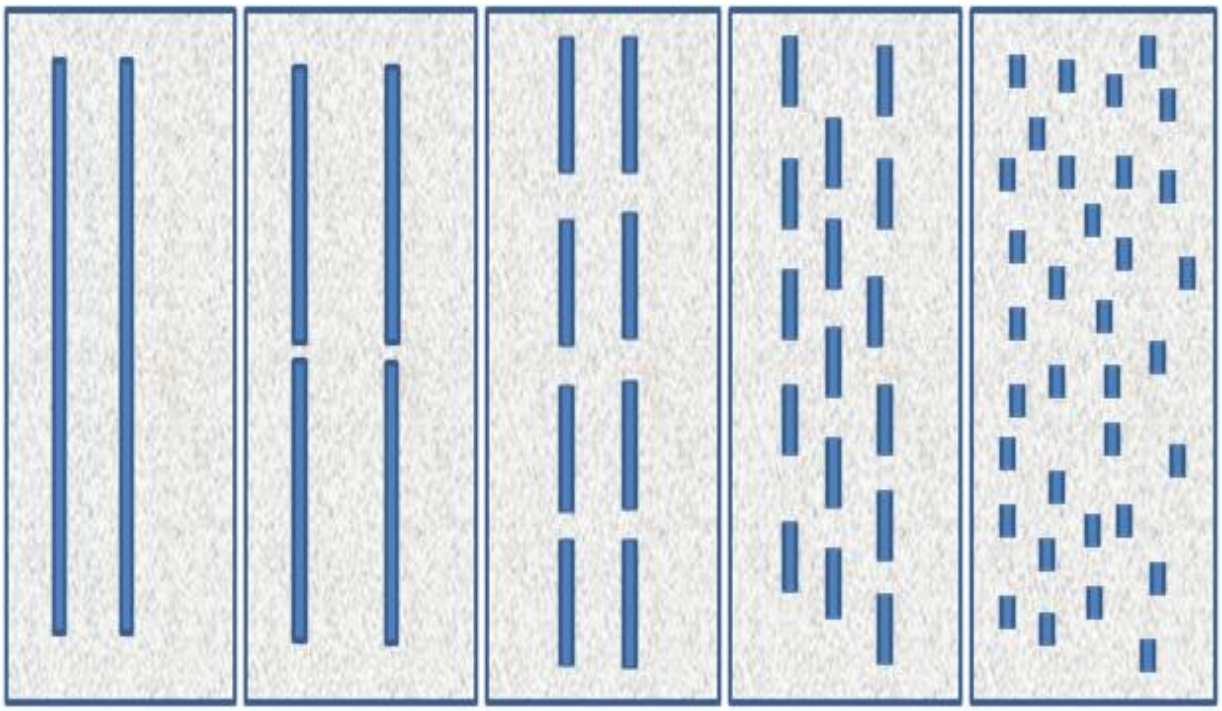

Figure 2.4. Schematic showing macropore distribution (connectivity) in the column for the 5.87% (D2) macropore system.

For a given porous media, the experiment was started without any macropores, and the hydraulic conductivity of the matrix was measured. The experiment was repeated to ensure the saturated hydraulic conductivity for the matrix was constant under conditions of repeated packing. For any given macropore density (D1 or D2) and inter-macropore connectivity (C1, C2, C3, C4, C5), artificial macropores were packed in to the column along with the bulk porous media such that the different inter-macropore connectivities were established (Figure 2.3 & 2.4). The column was packed randomly such that no macropore was open to the column boundaries and at the same time each of the macropores was separated from others. It was important to ensure that the macropores were not open to the ends of column because surface macropores and buried macropores are subject to different dynamics of flow. The column was also wet-packed to ensure air-tight conditions in the soil column and hydraulic conductivity was measured using the procedure described earlier. After the effective hydraulic conductivity was measured, the soil column with the artificial macropores was unpacked and subsequently, repacked with the same macropore density and connectivity, and a new effective hydraulic conductivity was measured.

Results and Discussion

Experiment study

For two types of macropore systems (Figure 2.5 and Figure 2.6), we observed similar effects of inter-macropore connectivity on hydraulic conductivity. As the macropores were made more discontinuous for a given macropore density, we found that the effective hydraulic conductivity of the porous media converged from a high value to the hydraulic conductivity of the bulk matrix. This change is especially significant for fine glassbeads, medium glassbeads, 40-60 sand and 12-20 sand. The 40-60 sand, which is the finest porous media we studied,

showed the most significant change. For macroporosity of 2.97%, the hydraulic conductivity of 40-60 sand increased from 3.52 cm/min (no-macropore condition) to 13.11 cm/min (highest inter-macropore connectivity). Similarly, for macropore density of 5.87%, the hydraulic conductivity of 40-60 sand changed from 3.52 cm/min to 18.14 cm/min in conditions of highest inter-macropore connectivity. It is also interesting to note that for conditions of least inter-macropore connectivity, the effective hydraulic conductivity of the porous media is very similar to the conductivity of the bulk matrix. This implies that from the perspective of hydraulics, the definition of what constitutes a macropore would depend on the connectivity of the macropores. In other words, one needs to carefully consider both physical (size) and morphological (arrangement) aspects to determine the influence of macropores in soils.

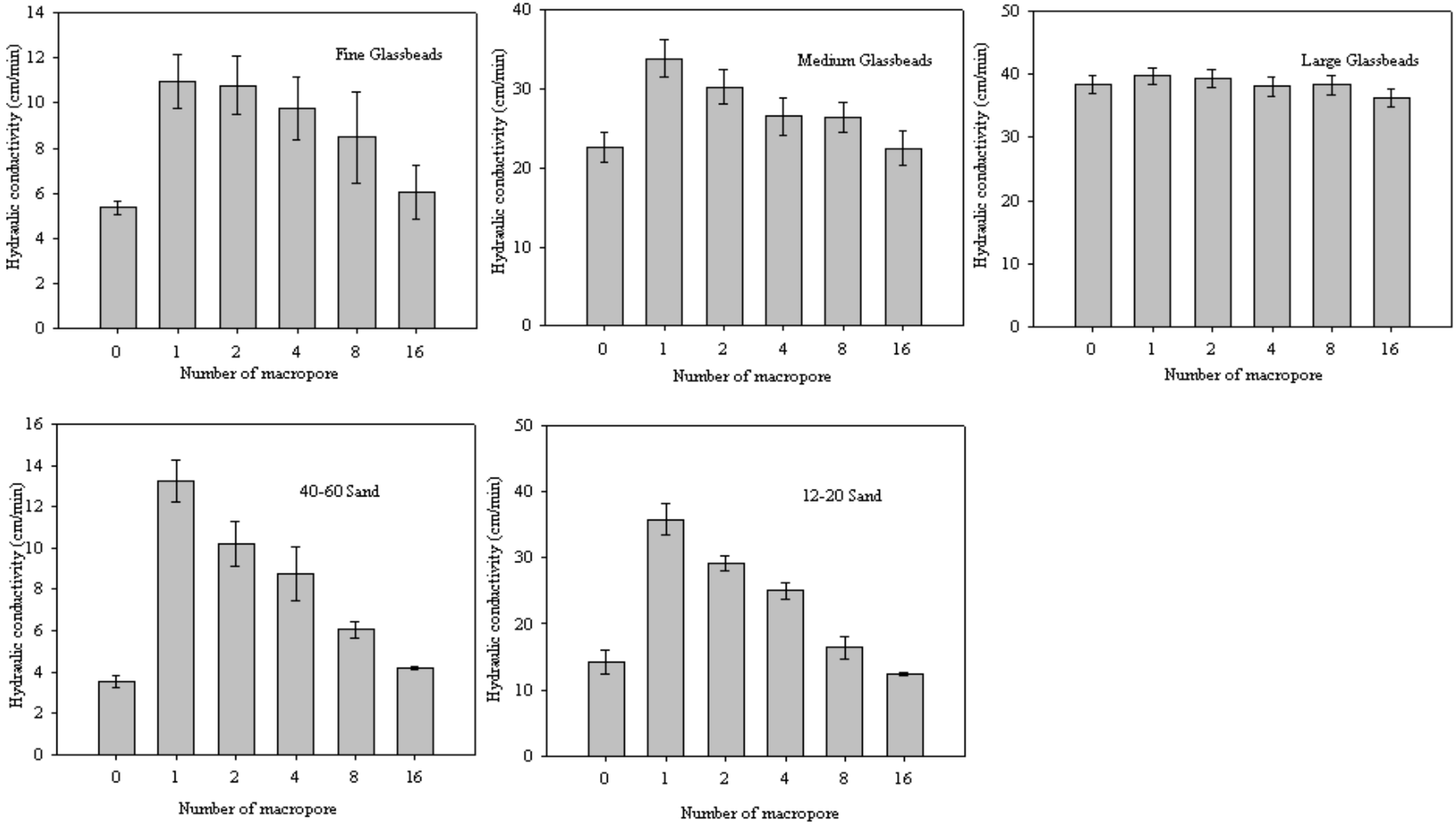

Fig 2.5. The relationship between hydraulic conductivity (cm/min) and the number of macropores for the 2.97% macropore system.

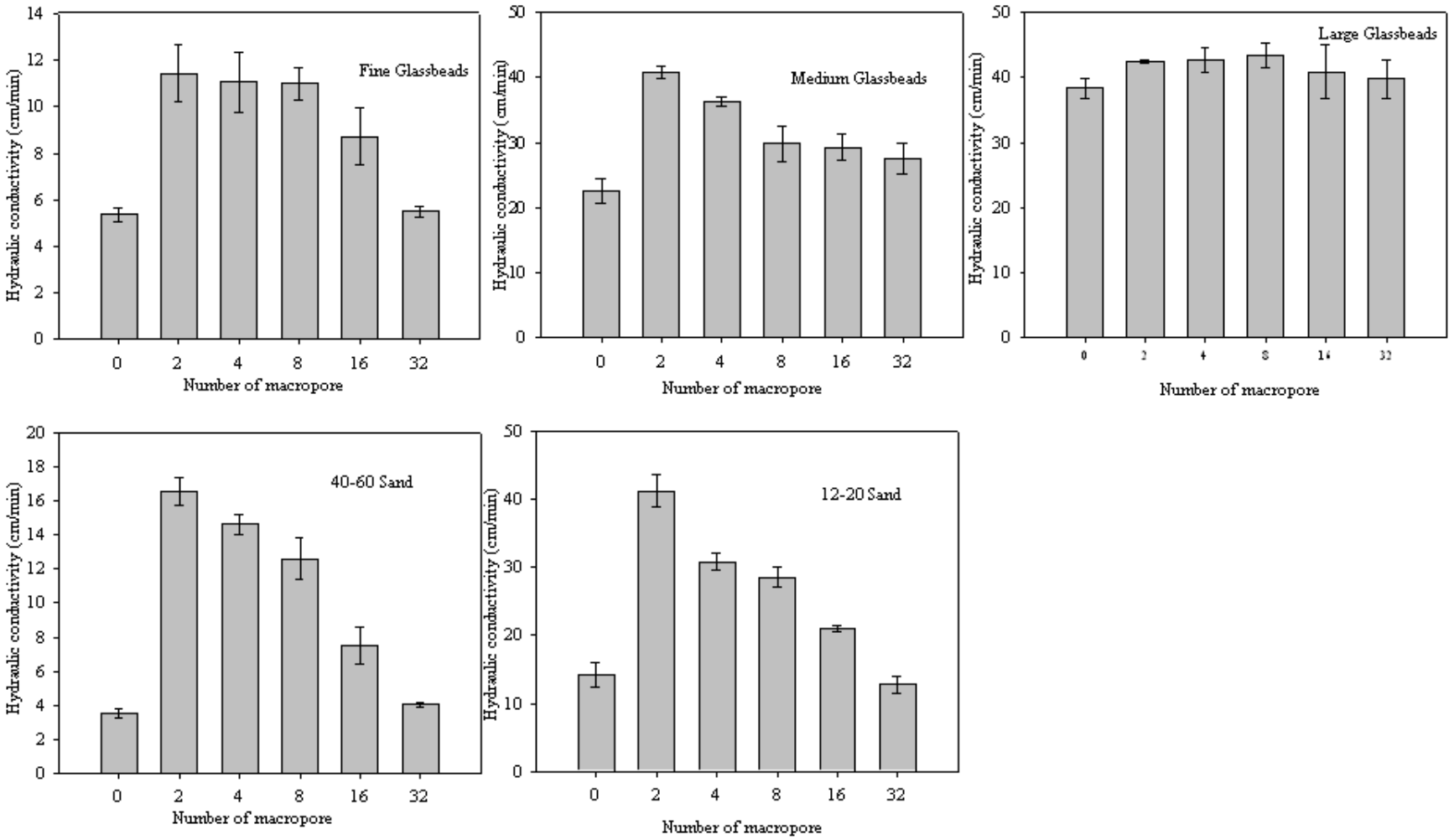

Fig 2.6. The relationship between hydraulic conductivity (cm/min) and the number of macropores for the 5.87% macropore system.

Comparing different porous media, it was observed that macropore connectivity has different effects on hydraulic conductivity that is based on the size of porous media. The effects of macroporosity are best observed when the size of the porous media is smallest. For example, in large glass bead media with a macroporosity of 2.97%, the hydraulic conductivity of the pure matrix without macropores is 38.36 cm/min while with macropores of highest connectivity (C1) is 39.70 cm/min. The extent of effects of macropore connectivity on the hydraulic conductivity decreases with coarser media, which implicate the properties of the porous medium also play a role on macropores effects. However, interplay between the definition of macropore (based on its size) and the effect of that macropore on soil hydraulic properties needs further analysis.

Numerical Modeling Study

For the bulk matrix, we used the saturated hydraulic conductivity from the experiments conducted for the non-macroporous condition. Assuming that Darcian-based flow concepts can be used to represent flow in matrix and the macropores (as used in dual-permeability models), we tried to estimate the hydraulic conductivity in the macropore domain that shows the best fit between the experimental and simulated effective saturated hydraulic conductivity of the porous media.

For a given macropore density and inter-macropore connectivity, the hydraulic conductivity in the macropore domain was estimated as follows: (a) artificially construct several macropore configurations using MATLAB, (b) using different possibilities of hydraulic conductivity in the macropore domain and experimentally measured value for the matrix, estimate the effective hydraulic conductivity by simulating constant-head method in MODFLOW. The MODFLOW domain used to represent the soil column used in the experiment was developed by dividing the diameter of the column in x and y directions in to 120 equally

spaced grids and the length of the column in to 180 equally spaced grids. We constructed several different macropore configurations (~10) using MATLAB for a given macropore density and inter-macropore connectivity in a porous media. Figure 2.7 shows an example of a macropore configuration generated for a macropore density of D1 (2.97%) and inter-macropore connectivity of (C1).

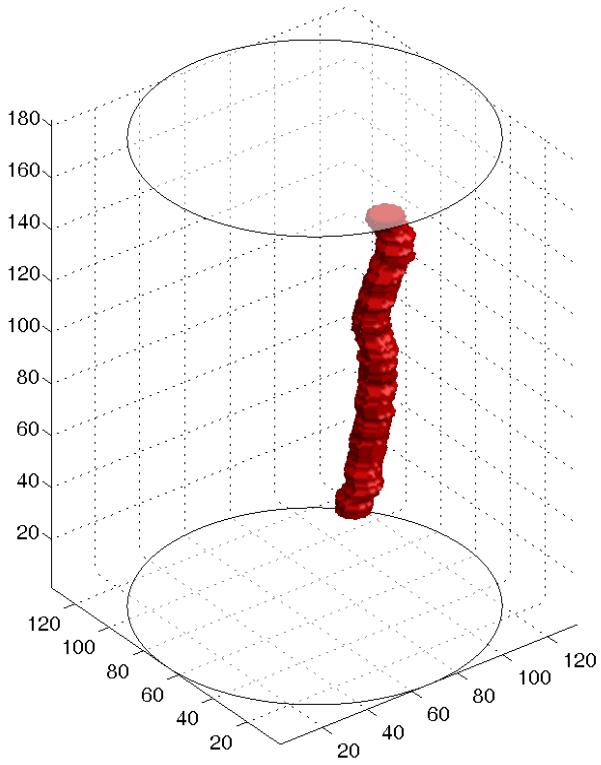

Fig 2.7. An example of a macropore configuration that was used in MODFLOW simulation to estimate the effective hydraulic conductivity in porous media at a macropore density of 2.97% with the best inter-macropore connectivity (C1).

Figure 2.8 shows the difference between the mean effective hydraulic conductivity that was measured experimentally and through MODFLOW simulations for a macropore density of 2.97% and inter-macropore connectivities considered in this study, in different porous media. Here, C1 represents the best connectivity of the macropore distribution in the column, and C5 represents the poorest connectivity of macropore distribution in the column. From C1 to C5, it can be observed that the macropores become more and more discontinuous. Figure 2.8 shows that for fine glassbeads and medium glassbeads, when the macroporosity is 2.97% the hydraulic conductivity of the macropore domain is around 850 cm/min, the simulation effective hydraulic conductivity of the column matches the experiment hydraulic conductivity of the column best (i.e. the experimental K minus simulated K approaches zero). For 40-60 Sand and 12-20 Sand, the hydraulic conductivity of the macropore domain is around 1700 cm/min, the simulation effective hydraulic conductivity of the column matches the experiment hydraulic conductivity of the column best.

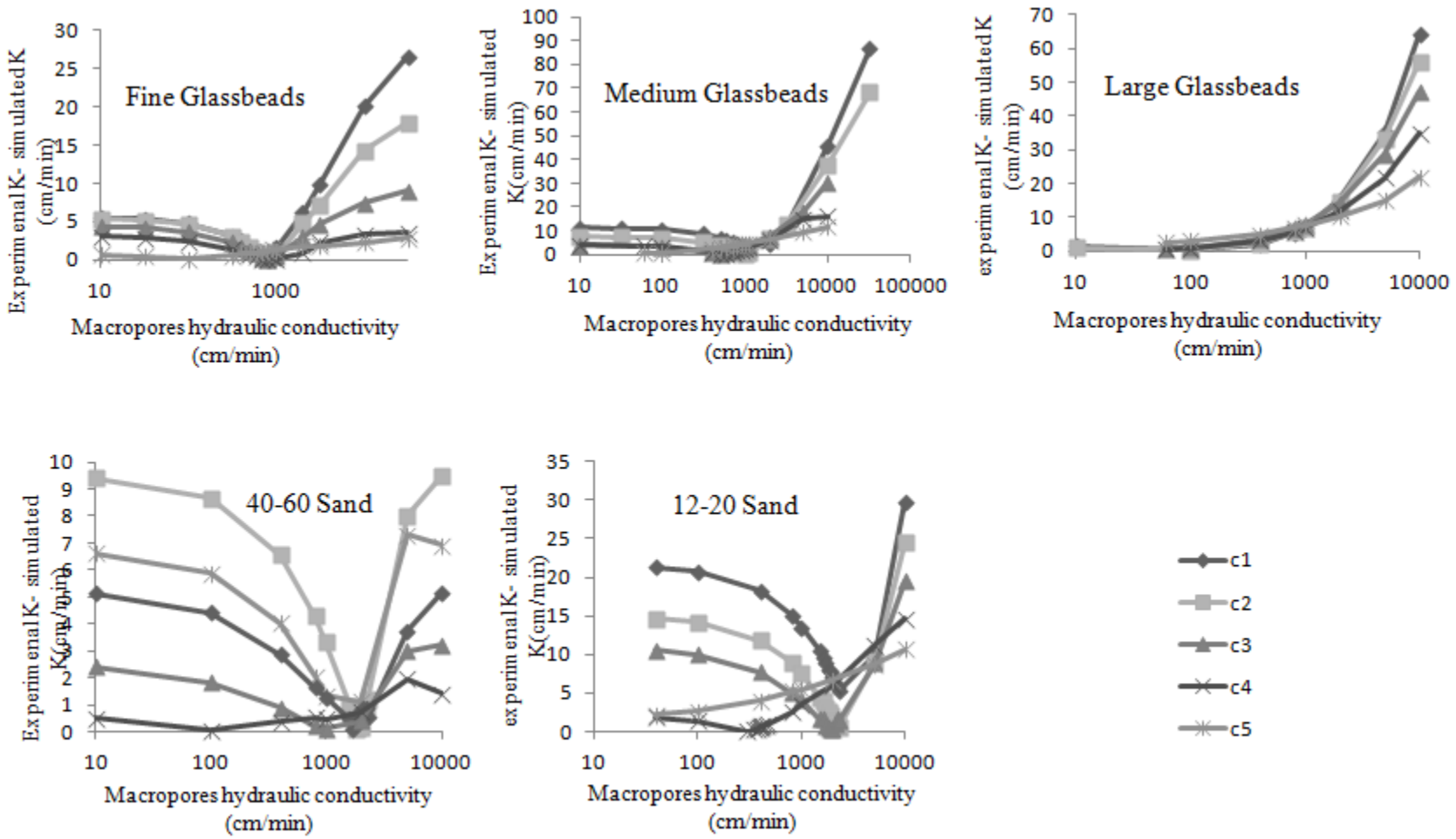

Figure 2.8. Relationship between hydraulic conductivity of macropore domain used in a MODFLOW simulation and the difference between the simulated and experimentally-estimated effective saturated hydraulic conductivity for a macropore density of 2.97%.

Summary and Conclusions

Macropores are very common in most soils and create preferential pathways for solute transport in the subsurface, which might reduce the availability of water and nutrients to plants, and cause accelerated transport of pollutants. Although many studies have been conducted to characterize the impact of macropore effects on saturated solute transport, applicability of the results from these studies is hampered by the fact that the structure of macropores in the field is often not known *a priori*. In this experimental investigation, we used artificial macropores to study the effects of macropore density and connectivity on the effective saturated hydraulic conductivity of porous media. The effective hydraulic conductivity of the porous media for different macropore distributions was analyzed using steady state water flow simulations. The results show that as macropores become discontinuous, the hydraulic conductivity approaches the value of no-macropore media. Also, the extent of effects of macropore connectivity on the hydraulic conductivity decrease when the porous media size was increased.

III. On understanding the Applicability of Darcy's Law Under High Velocity Conditions

Introduction

Water flow in porous media is traditionally modeled using Darcy's law described mathematically as shown in equation [3.1]:

$$q = -Ki$$

$$K = \frac{kg}{\gamma}$$

Where $\boldsymbol{q}$ is the flow rate per unit cross-section, also called as the specific discharge of water flow ($L^3/L^2/T$), $\boldsymbol{K}$ is the hydraulic conductivity of the porous media (L/T), $\boldsymbol{i}$ is the hydraulic gradient driving the flow, and $\boldsymbol{g}$ is the acceleration due to gravity (L/T^2). The hydraulic conductivity is related to the kinematic viscosity of the fluid, $\boldsymbol{\gamma}$ (L^2/T) and intrinsic permeability of the porous media, $\boldsymbol{k}$ (L^2) which describes the ability of the media to conduct flow (Equation 3.1b).

The linear relationship between the specific discharge and the gradient, as described by Darcy's law, has been found to be valid only under certain flow conditions (e.g., Dullien, 1992; Bear, 1988). Dullien (1992) best described the rationale behind Darcy's law as follows:

"The porous medium is imagined to be subdivided in to a network of small blocks, and Darcy's law is applied to each block. The size of each block must be small enough to approximate $\boldsymbol{q}$, $\boldsymbol{k}$, $\boldsymbol{i}$ *and* $\boldsymbol{\gamma}$ *with constant values within each block; but the size of each block must be large enough for Darcy's law in its macroscopic form to apply in the block."*

It is clear that Darcy's law is a close approximation of a complex set of physical process, but not a mathematical representation of the underlying processes. Previous researchers have described that the conditions under which the rationale described above is valid occurs under

laminar conditions (Bear, 1988). In fact, a linear approximation between gradient and the discharge is not uncommon in laminar flow in other regimes such as pipe flow. A laminar condition under which Darcy's law is valid can been defined mathematically using the Reynolds number (***Re***, dimensionless). For a porous medium, Reynolds number has been commonly estimated using the equation [3.2]:

$$\mathrm{Re} = \frac{qD}{\gamma}$$

where D is a characteristic length (L). This characteristic length is assumed often as the mean grain diameter. Although others have defined the characteristic length as other estimates of the grain size distribution, we use the mean grain diameter in this study.

The phenomenological nature of Darcy's law needs to be considered when applying the same in porous media applications. In the words of Freeze and Cherry (1979),

"Darcy's law is an empirical law. It rests only on experimental evidences".

Given the fact that Darcy's law has been ascribed to be an experimentally-derived than a fundamental law, defining the limitations of its use in porous media system is a worthy effort. For example, the threshold value (as represented by the highest Reynolds number) where Darcy's law may not be violated is not very clearly described. It is however, hypothesized to be dependent on the relative effects of viscous force and inertial forces in the porous media. It is commonly accepted that flow in porous media can be distinguished in to three zones (see Figure 3.1). The first zone, called as Darcian zone, corresponds to flow rates where the Darcy's law is a valid model. In this zone, viscous forces are dominant over the inertial forces in driving the flow. The upper limit of this zone is not clear and commonly assumed to be somewhere between Reynolds number of 1 and 10. The third zone corresponds to very high Reynolds numbers where

the flow is turbulent. Lindquist (1930) suggested that the hydraulic gradient in the third zone is linearly related to the Reynolds number (or quadratic with respect to specific discharge). Inertial force dominates viscous forces leading to turbulent flows. The second zone is transitional in nature and lies between the first and third zones. In most practical situations involving flow in porous media, one may not expect to exceed Reynolds number of more than 10 with a majority of them not exceeding Reynolds numbers of 1 (Firdaouss et al., 1997). Hence, our interest lies in characterizing flow in the Darcian zone and transition zones.

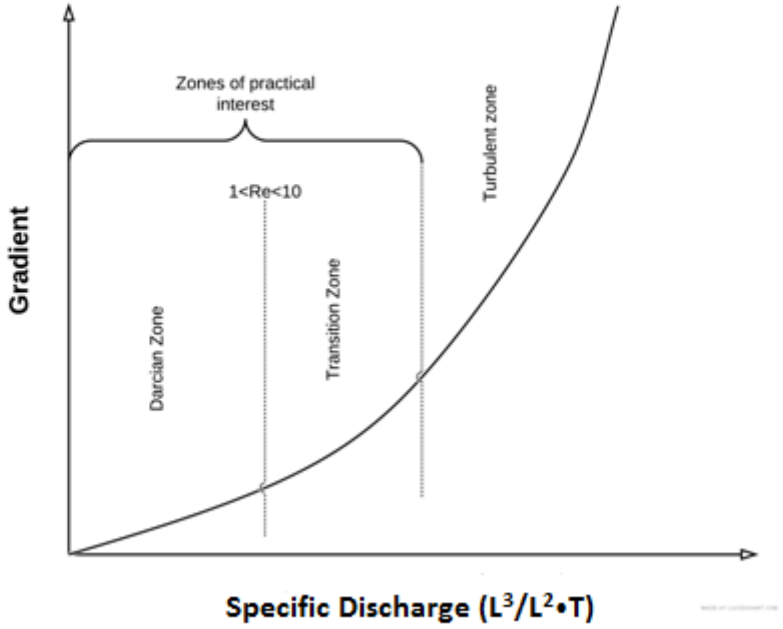

Figure 3.1. Schematic of specific discharge vs gradient relationship (Bear 1972).

In an effort to mathematically represent the transition of flow in porous media from Darcian regime in to the transition zone and beyond, several authors have proposed non-linear extensions of Darcy's law (Dullien, 1992; Firdaouss et al., 1997 etc.). Most of these non-linear variations of Darcy's law resemble a quadratic form as shown in equation [3.3].

$$i = \alpha q + \beta q^2$$

The constant, α represents the linearity of flow in the porous media (inversely proportional to the hydraulic conductivity) and β represents the non-linearity that is induced in the transition zone. Probably, the best known equation of this form is the Ergun Equation (Ergun, 1952). Using the Ergun equation, the values of constants α and β can be estimated from the properties of porous media as shown below:

$$\alpha = \frac{A\mu}{\rho g}\left(\frac{(1-\phi)^2}{\phi^3 D^2}\right)$$

$$\beta = \frac{B}{g}\left(\frac{(1-\phi)}{\phi^3 D}\right)$$

where ϕ is the porosity, A and B are constants assumed to be 180 and 1.8 (or 4.0) for most media and D is the average diameter of the particles in the porous media that is representative of the characteristics length. MacDonald et al. (1979) tested the Ergun equation for an extensive set of porous media and found that the Ergun equation can make reasonable predictions for flow dynamics in the porous media systems.

While equations such as the Ergun's equation can describe non-linear effects of flow in porous media across the Darcian, transition and turbulent zones, a number of drawbacks can be

observed from the standpoint of making hydrological predictions using this equation. The model does not lead it to formulation of governing equations in porous media that exhibit non-darcian characteristics. Hydrogeologists are used to representing discharge as a function of hydraulic gradient unlike chemical engineers who are more interested in estimating gradient as a function of specific discharge. As a consequence, formulations such as Equation [3.3] are biased towards representing the turbulence in flow through porous media as they are developed mostly by chemical scientists. On the other hand, hydrogeologists focus on the Darcian and transition zones. We believe that one can develop better intuitive equations that lend themselves better to modeling flow through porous media in the Darcian and transition zones. The objective of this paper is two-fold: (a) to understand the limitations of Darcy's law as a function of porous media and (b) to develop a intuitive equation for describing the non-linear effects on flow through porous media that is better suited for modeling hydrogeological system.

Theoretical Analysis

Derivation of the Inverted Ergun Equation

The Ergun equation, as shown in equation [3.3], describes the relationship between the hydraulic gradient and the specific discharge. Rewriting equation [3.3], we get

$$\frac{i}{\beta} = \frac{\alpha}{\beta} q + q^2 \Rightarrow \frac{i}{\beta} + \frac{\alpha^2}{4\beta^2} = \frac{\alpha^2}{4\beta^2} + 2\left(\frac{\alpha}{2\beta}\right) q + q^2$$

$$\left(q + \frac{\alpha}{2\beta}\right)^2 = \frac{i}{\beta} + \frac{\alpha^2}{4\beta^2}$$

Simplifying further, we get

$$\left(q+\frac{\alpha}{2\beta}\right) = \left(\frac{i}{\beta}+\frac{\alpha^2}{4\beta^2}\right)^{\frac{1}{2}} \Rightarrow q = \frac{\alpha}{2\beta}\left(\left(\frac{4i\beta}{\alpha^2}+1\right)^{\frac{1}{2}}-1\right)$$

In mathematics, a Taylor series is a representation of a function as an infinite sum of terms that are calculated from the values of the function's derivatives at a single point (Abramowitz and Irene 1970). One of the Taylor series expansions is as follow:

$$\sqrt{1+x} = \sum_{n=0}^{\infty} \frac{(-1)^n(2n)!}{(1-2n)(n!)^2(4^n)}x^n = 1+\tfrac{1}{2}x-\tfrac{1}{8}x^2+\tfrac{1}{16}x^3-\tfrac{5}{128}x^4+\ldots \text{ for } |x| \leq 1$$

Under conditions of $\frac{4i\beta}{\alpha^2} \leq 1$,

Equation [3.6] can be simplified using Taylor's series expansion up to the cubic term as follows:

$$q = \frac{\alpha}{2\beta}\left(\left(\frac{4i\beta}{\alpha^2}+1\right)^{\frac{1}{2}}-1\right) = \frac{\alpha}{2\beta}\left(\frac{1}{2}\left(\frac{4i\beta}{\alpha^2}\right)-\frac{1}{8}\left(\frac{16i^2\beta^2}{\alpha^4}\right)+\frac{1}{16}\left(\frac{64i^3\beta^3}{\alpha^6}\right)\right)$$

$$q = \frac{i}{\alpha}i-\frac{\beta}{\alpha^3}i^2+2\frac{\beta^2}{\alpha^5}i^3$$

$$q = \eta i + \lambda i^2 + \chi i^3$$

where $\eta = \frac{1}{\alpha}$, $\lambda = -\frac{\beta}{\alpha^3}$ and $\chi = 2\frac{\beta^2}{\alpha^5}$. The derived equation, hereby called as the Inverted Ergun (IE) equation, represents the discharge-hydraulic gradient relationships beyond the Darcian zone. The IE equation can be visualized as comprising of a linear component (ηi) that is Darcian in nature and two non-linear terms ($\lambda i^2 + \chi i^3$) that models the flow transition away from

the Darcian zone. It may be observed that the IE equation is more intuitive than the Ergun equation. Another advantage of the IE equation is that it preserves the use of all the parameters used in the Ergun equation and does not introduce any new parameters of its own. Thus, the equation can be readily applied using parameter information available in the literature.

Validity of the Inverted Ergun's Equation

For equation [3.9] to be valid, equation [3.7] has to be satisfied. It is possible to estimate the maximum hydraulic gradient i_{ie} until which the IE equation is valid. The limiting gradient i_{ie} is defined from eqn 3.7 as $i_{ie} = \alpha^2 / 4\beta$ and substituting the values of α and β from eqn. 3.4 a&b , we get

$$i_{ie} = \frac{\alpha^2}{4\beta} \quad \Rightarrow i_{ie} = \frac{A^2 \mu^2 (1-\phi)^3}{4 g \rho^2 B \phi^3 D^3}$$

In equation [3.10], the hydraulic gradient up to which Equation [3.9] is valid (i_{ie}) is shown to be a function of the mean grain size diameter of the porous media and the porosity. Figure 3.2 shows hydraulic gradient-specific discharge relationships estimated using Ergun and Inverted Ergun equations for a variety of average grain sizes. Figure 3.3 shows variation of i_{ie} as a function of porosity and average grain sizes diameter. The values of i_{ie} for the different grain sizes shown in Figure 3.3 are rarely encountered in practical hydrological application and therefore, one could conclude that IE should be adequate for practical applications.

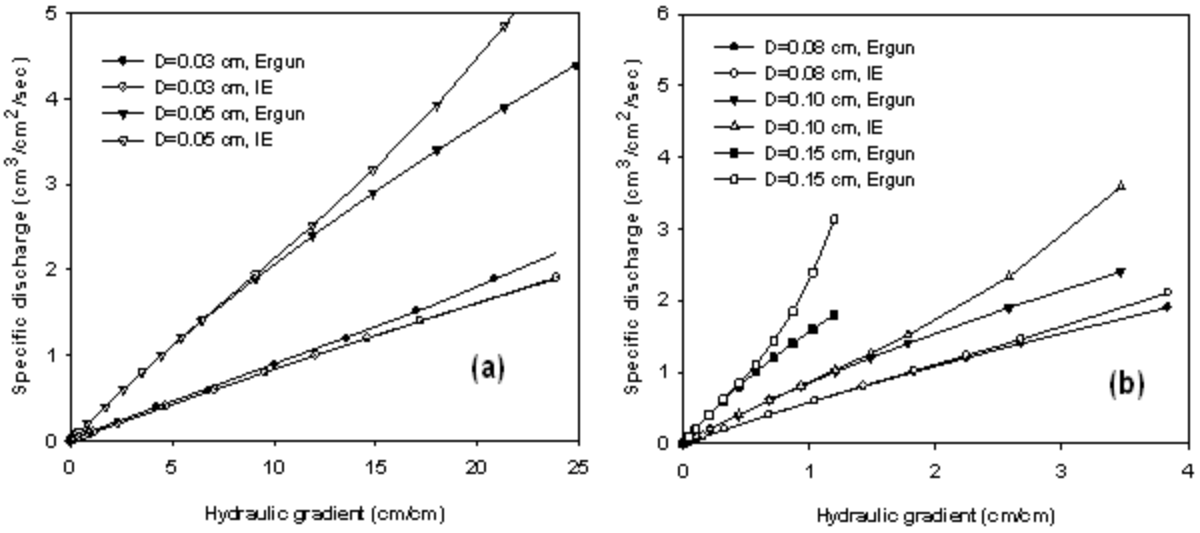

Figure 3.2. An illustration of the gradient-specific discharge relationships as estimated by the Ergun (solid symbols) and Inverted Ergun Equations (IE, open symbols) (assuming constants, A=180 and B=1.80 and porosity of 0.40). Plot (a) shows the curves for average grain diameters of 0.08(square), 0.10(triangle) and 0.15 cm (circle). Plot (b) shows the curves for average grain diameters of 0.03(circle) and 0.05(triangle).

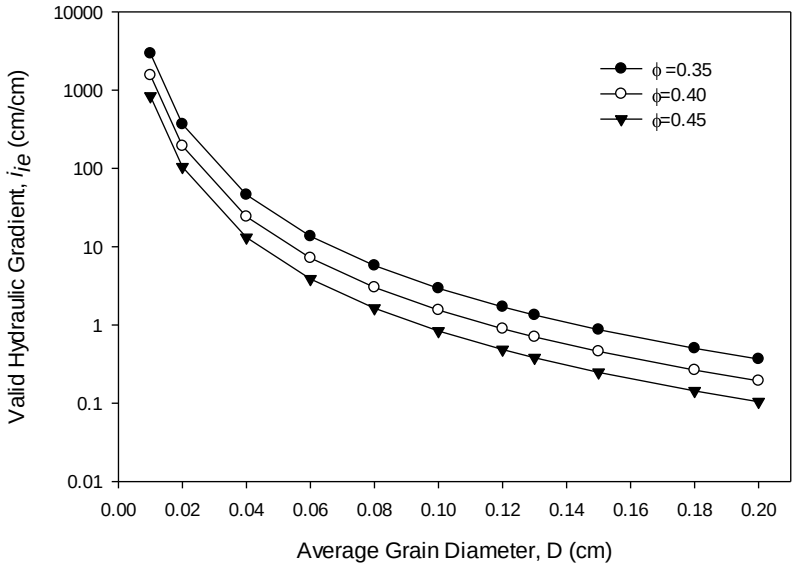

Figure 3.3. Variation of maximum hydraulic gradient as a function of mean grain size diameter (cm) at various porosities, ϕ **(**cm^3/cm^3) values (assuming constants, A=180 and B=1.80 and using the inverted Ergun equation).

Defining the Upper Limit for the Validity of Darcy's Law

It has long been recognized that the upper limit of velocity until which Darcy's law is valid is unclear (Bear 1988). Although a Reynolds number of 1-10 has been suggested to be the upper limit, this range is too wide to be used. Also, for subsurface hydrology application, it would be more intuitive to express this upper limit as a function of hydraulic gradient and porous media. Specific discharge-hydraulic gradient relationships are essentially non-linear across all values of hydraulic gradient. This is especially the case for coarser soils. We propose that the gradients (or Reynolds number) up to which Darcy's law is valid should be statistically defined rather than on a purely physical basis. This is largely due to the fact that a physical approach to estimating the upper limits of validity for Darcy's law would attempt to linearize a phenomenon which is essentially non-linear. We propose that the hydraulic gradient up to which Darcy's law is valid should depend on the maximum error that one is willing to accept in the resulting estimates of specific discharge.

Mathematically, deviations from Darcy's law at larger hydraulic gradients are observed because of significant contributions from the non-linear component of the inverted Ergun's equation as compared to its linear component. Therefore, as long as the non-linear components does not exceed by a certain percentage compared to the linear component of the equation, Darcy's law can be assumed to be valid. If ε is the acceptable fractional error which is a ratio of the non-linear terms in the IE equation (quadratic and cubic terms) and the linear term, as defined as below:

$$\left|\frac{(\lambda i^2 + \chi i^3)}{\eta i}\right| \leq \varepsilon$$

Let us define i_d is the limiting gradient at which eqn. 3.11 (a) be statisfied as

$$\frac{\lambda i^2 + \chi i^3}{\eta i} = \varepsilon$$

The above equation can be arranged as:

$$\frac{\beta}{\alpha^3} i_d^{\,2} - 2\frac{\beta^2}{\alpha^5} i_d^{\,3} = \varepsilon \frac{i_d}{\alpha} \qquad \Rightarrow i_d = \frac{\alpha^2}{\beta}\left(\frac{1-\sqrt{1-8\varepsilon}}{4}\right)$$

where i_d is the maximum hydraulic gradient up to which Darcy's law may be considered to be valid. It may be observed that $i_{d\ \text{has}}$ a very similar mathematical form as i_{ie}. Combining equations [3.10] and [3.11], we get

$$i_d = \left(1-\sqrt{1-8\varepsilon}\right) i_{ie} = \frac{A^2\mu^2(1-\phi)^3}{4g\rho^2 B\phi^3 D^3}\left(1-\sqrt{1-8\varepsilon}\right)$$

Therefore, the maximum hydraulic gradient up to which Darcy's Law is not violated will always be less than the hydraulic gradient up to which the Inverted Ergun's equation. Equation [3.12] proves that the IE equation can adequately represent the flow in porous media for Darcian ($0<i<i_d$) and transition zones ($i_d<i<i_{ie}$) that one typically observes in ground water flow regimes. For a given porous media, the maximum Reynolds number (Re_d) at which the Darcy's law is not valid can be calculated as follows:

$$\mathrm{Re}_d = \frac{q_d \rho D}{\mu} \approx \frac{(\eta i_d)\rho D}{\mu} = \frac{(\frac{\alpha}{\beta}\left(\frac{1-\sqrt{1-8\varepsilon}}{4}\right))\rho D}{\mu} = \frac{\alpha\rho D\left(1-\sqrt{1-8\varepsilon}\right)}{4\beta\mu}$$

$$\mathrm{Re}_d = \frac{\left(1-\sqrt{1-8\varepsilon}\right)A(1-\phi)}{4B}$$

Figure 3.4 shows the variation in $\mathrm{Re_d}$ as a function of A/B and the acceptable error. It is interesting to note that Reynolds number up to which Darcy's law is valid is truly dependent only on the porosity of the porous media (or the bulk density of the porous media). Strikingly, MacDonald (1979) in his extensive review of available literature data suggested that deviations from Darcy's law seem to become noticeable in the range of $\mathrm{Re_d}/\ (1-\phi)$ ~1-10.

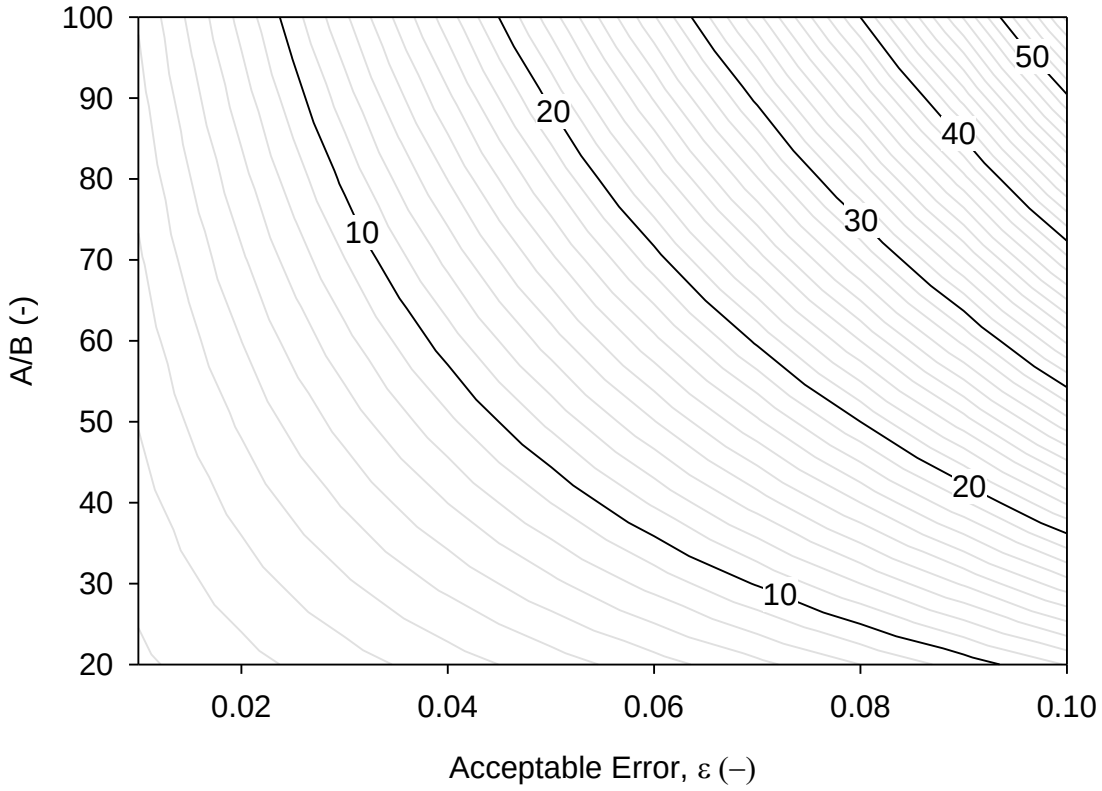

Figure 3.4. Contour of the maximum Reynolds number ($\mathrm{Re}_d = \frac{\left(1-\sqrt{1-8\varepsilon}\right)A(1-\phi)}{4B}$) as a function of the relative error (**ε**) and the system parameter A/B.

Experimental Method

MacDonald et al. (1979) provides a comprehensive review of experimental data available in the literature that describes flow dynamics in porous media. Although extensive data is available that show hydraulic gradient-specific discharge relationships for a variety of porous media, they were collected with an intention to characterize the turbulent zone. However, for subsurface hydrology applications, it is necessary to gather/ develop datasets that focus on the Darcian and transition zones and characterize the transition between the two zones. Due to lack of such datasets, we designed new set of experiments to develop hydraulic gradient-specific discharge relationships for a variety of glass beads and sands. Table 3.1 lists the properties of the porous media used in our experiments. The experimental setup was based on the 'constant head' approach for estimating hydraulic conductivity. Figure 3.5 shows a schematic of the experiment. Soil was packed in to the bottom 30 cm of a long graduated glass cylinder of 3.64 cm diameter under saturated conditions. Degassed water was used at all times to ensure complete saturation of the column. The bottom of the soil column was connected to a stationary outlet where flow rates were measured. The outlet was elevated such that the soil column remains saturated under static conditions. A peristaltic pump (Master flex) was used to continuously pump water in to the column and head at the top of the soil column was controlled using a movable outlet that was connected to the glass cylinder just above the soil column. By moving the outlet using a pulley mechanism, head at the top of soil column was fixed at various desired values. The head measurements were directly read on the cylinder to avoid any measurement errors. All inflow and outflow waters were delivered through a reservoir that re-circulated the degassed water to ensure a closed system.

Name	G1	G2	G3	S1	S2	S3
Type of porous media	Glassbeads	Glassbeads	Glassbeads	Sand	Sand	Sand
Average grain diameter (cm)	0.19	0.15	0.05	0.11	0.06	0.03
Particle density (g/cm^3)	2.47	2.49	2.49	2.63	2.62	2.76
Porosity [1]	0.36	0.37	0.33	0.34	0.33	0.36
Number of Data points	34	30	45	43	51	45
Range of Re	0	0-15.6	0-6.25	0-14.46	0-11.8	0-4.2
Range of Hydraulic gradients	0-1.81	0-1.94	0-9.29	0-4.39	0-6.42	0-12.64
Range of specific discharge	0-1.31	0-1.38	0-0.66	0.1.31	0-1.39	0-0.96

Table3.1 Properties of porous media used and a summary of the related experiment performed to develop gradient-specific discharge data for this study. G1 is Large Glassbeads, G2 is Medium Glassbeads, G3 is Fine Glassbeads, S1 is No. 12-20 Sand, S2 is No.20-40 Sand and S3 is No.40-60 Sand.

1. Calculated from measured bulk density (Gravimetric method (SSSA, 2002b) and particle density (Liquid displacement method (SSSA, 2002b)).

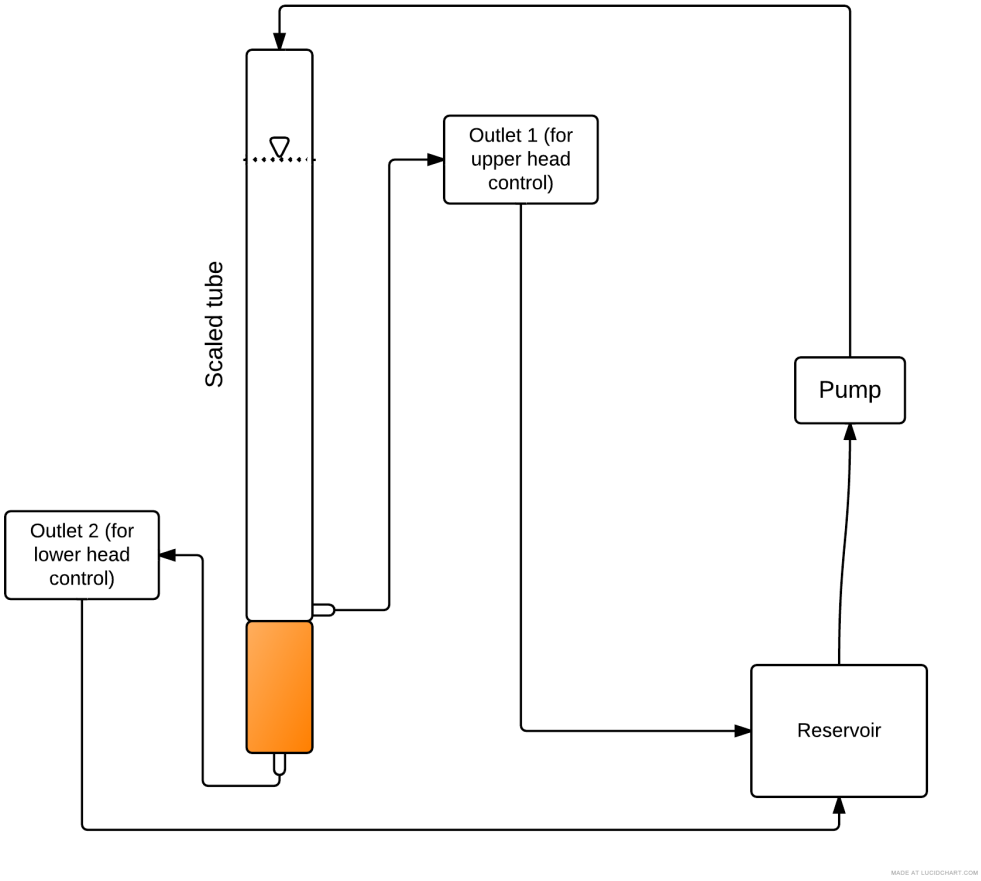

Figure 3.5(a) Experimental setup for estimating specific discharge-gradient relationships. Soil was packed in to the bottom 30cm of a long graduated glass cylinder of 3.64 cm diameter under saturated conditions.

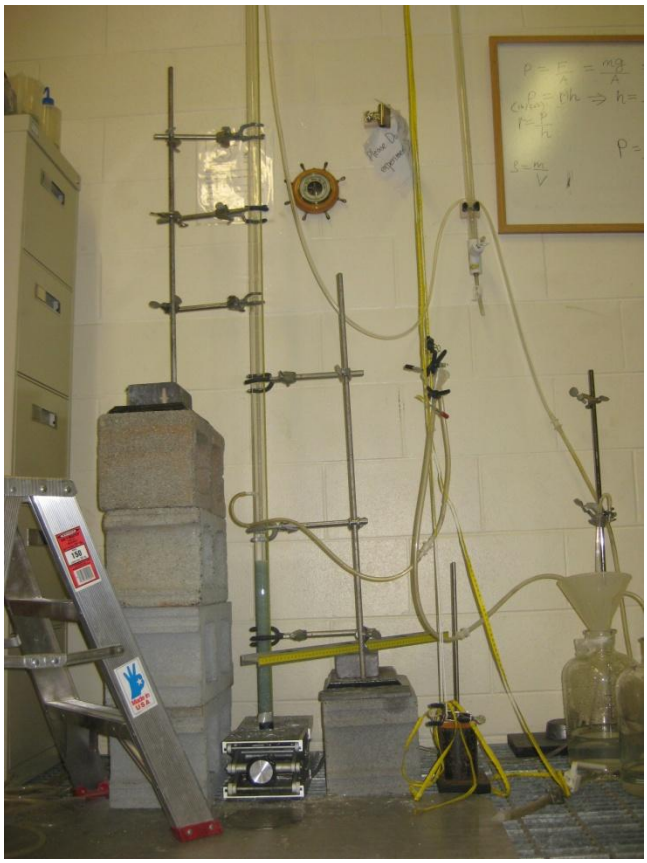

Figure 3.5(b) Pictures of experimental setup for estimating specific discharge-gradient relationships. Soil was packed in to the bottom 30cm of a long graduated glass cylinder of 3.64 cm diameter under saturated conditions

Analysis of Experimental Results

Experimental data was collected for the porous media under consideration using the setup explained in the previous section. Figure 3.6 and 3.7 shows the relationships between specific discharge and hydraulic gradient for glass beads and sands respectively. One may clearly notice a quadratic nature in these relationships. On preliminary examination, it is conceivable that there exists a gradient for at least some of these porous media where the quadratic nature of the specific discharge-hydraulic gradient may violate Darcy's law.

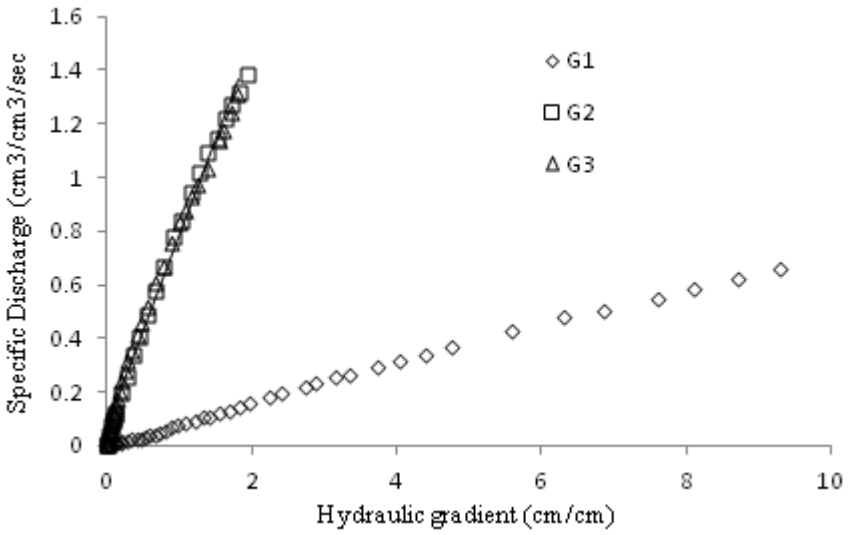

Figure 3.6. Experimental data for measured hydraulic gradient and the specific discharge for all three glassbeads. G1 is Large Glassbeads, G2 is Medium Glassbeads, and G3 is Fine Glassbeads.

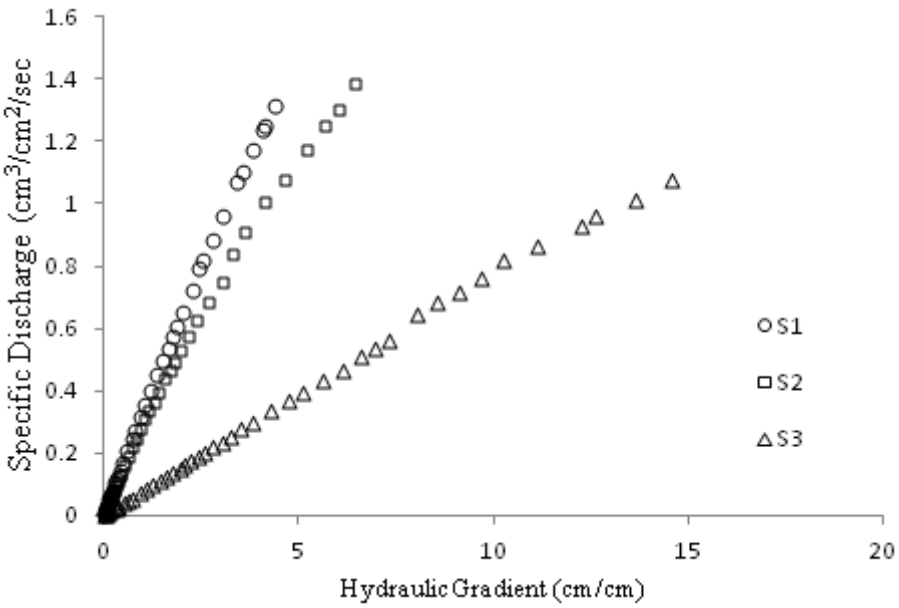

Figure 3.7 Experimental data for measured hydraulic gradient and the specific discharge for all three silica sands. , S1 is No. 12-20 Sand, S2 is No.20-40 Sand and S3 is No.40-60 Sand.

Using the data obtained from the experiments for different porous media, we analyzed the effectiveness of the following: (a) Coefficients in the Ergun equation by directly curve-fitting the dataset, (b) Coefficients from Ergun coefficients obtained in (a), (c) Coefficients estimated by directly curve-fitting the dataset (IE_c). We observed that the IE equation coefficients estimated using curve-fitting and using Ergun coefficients were similar in magnitude. Hence, we reported only the IE coefficients estimated through curve fitting. Table 3.2 lists the Ergun and IE coefficients estimated through curve-fitting. One may notice that the non-linear coefficients tend to get smaller as the porous media is more coarser. Table 3.2 also reports the gradients up to which the IE equation and the Darcy's equation is valid for these porous media.

Type of porous media	G1	G2	G3	S1	S2	S3
α *(sec/cm)*	0.31	0.95	11.47	0.85	1.61	11.47
β *(sec^2/cm ^{2})*	0.23	0.11	0.57	0.35	0.48	1.27
η (-)	3.27	1.05	0.09	1.17	0.62	0.09
λ(-)	-8.13	-0.13	0.001	-0.56	-0.11	0.003
χ (-)	40.41	0.03	0.002	0.53	0.04	0.002
i_{ie}	0.10	1.98	57.34	0.52	1.36	25.80
i_d *(for* ε=0.1)	0.04	0.79	22.94	0.21	0.54	10.32
Estimated the Value of A	155.08	148.30	175.40	165.30	193.40	184.30
Estimated the Value of B	4.00	1.80	1.80	3.90	5.60	2.20

Table 3.2 Estimated values of Ergun and inverted Ergun coefficients for the porous medium used in the experimental study. α represents the linearity of flow in the porous media.
Notes:
G1 is Large Glassbeads, G2 is Medium Glassbeads, G3 is Fine Glassbeads, S1 is No. 12-20 Sand, S2 is No.20-40 Sand and S3 is No.40-60 Sand.
β represents the non-linearity that is induced in the transition zone.
$\eta = \frac{1}{\alpha}$, $\lambda = -\frac{\beta}{\alpha^3}$ and $\chi = 2\frac{\beta^2}{\alpha^5}$.
i_{ie} is the maximum hydraulic gradient until which the IE equation is valid.
i_d is the maximum hydraulic gradient up to which Darcy's law may be considered to be valid.
A and B are porous media properties.

We have developed and showed the applicability of an equation to determine the upper limit for the validity of Darcy's equation.

From the coefficients estimated for IE equation, we inverse-estimated the values of parameters A and B for these porous media. We observed that estimates of A and B are estimated to be in the range of 140-200 and 1-6 respectively. These are also the suggested range for these parameters in the literature (Dullien, 1992).

Summary and Conclusions

Darcy's Law is not an exact mathematical representation for porous media flow, instead it is an empirical approximation of the underlying physical processes. The threshold value of hydraulic gradient above which the Darcy's law may be violated was investigated. By modifying the Ergun equation, a new expression has been suggested that can represent the discharge-hydraulic gradient relationship beyond the Darcian zone. Using this equation an estimate of maximum hydraulic gradient up to which Darcy's Law is not violated has been calculated. It was interesting to observe that the validity of the Darcy's law depends purely on the porosity and this theoretical finding is consistent with empirical observations made in the past. For example, MacDonald (1979) reviewed all available literature data and suggested that deviations from Darcy's law would be noticeable when $Re_d/(1-\phi)$ ~1-10. Our theoretical model also yielded similar constrains for the validity of Darcy's Law.

IV. Recommendations for Future Work

Biopores in soils can have a well structured pattern and can spread quite extensively throughout the subsurface. The size, distribution, continuity, depth as well as hydraulic characteristics of biopores can vary as a function of hydrological conditions as well as behavioral characteristics of the burrowing animal. A number of burrowing animals create macropores in soils for different depths and connectivities, which is much more complicated than the structure created by artificial macropores in lab. Biopores created by burrowing animals and invertebrates have significant influence on hydrological process. It is recommended that future investigations should combine the results of this effort with the knowledge of other disciplines such as entomology to better characterize various types of realistic biopores expected to be present in natural systems. This would help us develop a better understand of the impacts of biopores on water storage, solute transport in porous media systems. Such a fundamental understanding will help us better describe large-scale hydrological processes such as infiltration and runoff .

References

Abramowitz Milton; Stegun Irene A. 1970. Handbook of Mathematical Functions with Formulas, Graphs, and Mathematical Tables, New York: Dover Publications, Ninth printing.

Addiscott, T.M., Brockie, D., Catt, J.A., Christian, D.G., Harris, G.L., Howse, K.R. et al. 2000. Phosphate losses through field drains in a heavy cultivated soil. Journal of Environmental Quality, 29, 522–532.

Ahuja, L.R. 1993. Characteristics of macropore transport studied with the ARS Root Zone Water Quality Model. Transactions of ASAE. 36:369–380.

Bear, J. 1972. Dynamics of Fluids in Porous Media. American Elsevier Publishing Company, New York.

Beven, K., 1991. Modeling preferential flow: an uncertain future? In: Gish, T.J., Shirmohannadi, A. (Eds.), Preferential Flow, American Society of Agricultural Engineers, St Joseph, MI, pp. 1–11.

Beven, K., and P. Germann, 1982, Macropores and water flow in soils, Water Resource Reserach. 18, 1311-1325.

Blake, G., Schlichting, E. and Zimme rman, U,1973. Water recharge in a soil with shrinkage cracks. Soil Science Society of American Journal. In Proc., 37: 669-672.

Bouma, J.,1981. Soil morphology and preferential flow a long ma cropores. Agricultural Water Management. 3:235-250.

Brewer, R., 1964. Fabric and Mineral Analysis of Soils, John Wiley, New York.

Bullock, P. and Thomasson,A.J., 1979. Rothamsted studies of soil structure. II. Measurement and characterization of macroporosity by image analysis and comparison with data from water retention measurements. Journal of Soil Science, 30: 391--413.

Bundt, M., Widmer, F., Pesaro, M., Zeyer, J. & Blaser, P. 2001b. Preferential flow paths: biological 'hot spots' in soils. Soil Biology and Biochemistry, 33, 729–738.

Camobreco, V.J., Richards, B.K., Steenhuis, T.S., Peverly, J.H. & McBride, M.B. 1996. Movement of heavy metals through undisturbed and homogenized soil columns. Soil Science, 161, 740–750.

Capowiez, Y., Monestiez, P. & Belzunces, L. 2001. Burrow systems made by Aporrectodea nocturna and Allolobophora chlorotica in artificial cores: morphological differences and effects of interspecific interactions. Applied Soil Ecology, 16, 109–12.

Chertkov, V.Y. & Ravina, I. 1999. Tortuosity of crack networks in swelling clay soils. Soil Science Society of America Journal, 63, 1523–1530.

Childs, E.C. 1969. An Introduction to the Physical Basis of Soil Water Phenomena. J. Wiley & Sons, London.

David E. Radcliffe. 2008, Water and Solute Movement, 1048-1050, CRC Press.

Dullien, F.A.L., 1992. Porous Media, Fluid Transport and Pore Structure, Academic Press, San Diego.

Dykhuizen, R. C., 1987, Transport of solutes through unsaturated fractured media, Water Research, 21, 1531-1539.

Edwards, W.M., Shipitalo, M.J., Traina, S.J., Edwards, C.A. & Owens, L.B. 1992. Role of Lumbricus terrestris (L.) burrows on quality of infiltrating water. Soil Biology and Biochemistry, 24, 1555–1561.

Edwards, W.M., Norton, L.D. & Redmond, C.E. 1988. Characterizing macropores that affect infiltration into nontilled soil. Soil Science Society of America Journal, 52, 483–487.

Ehlers, W., 1975. Observation on earthworm channels and infiltration on tilled and untilled loess soil. Soil Science, 119: 242--249.

Ela, S.D., Gupta, S.C., Rawls, W.J. & Moncrief, J.F. 1991. Role of earthworm macropores formed by Aporrectodea tuberculata on preferential flow of water through a Typic Hapludoll. In: Preferential Flow (eds T.J. Gish & A. Shirmohammadi), pp. 68–76. Proceedings of the National Symposium, December 1991. American Society of Agricultural Engineers, Chicago.

Elliott, E.T. & Coleman, D.C. 1988. Let the soil work for us. Ecological Bulletins, 39, 23–32.

Ergun, S. 1952, Fluid flow through packed columns. Chemical Engineering Progress, 48, 89-94.

FOCUS 2001.FOCUS Surface Water Scenarios in the EU Evaluation Process Under 91/414/EEC. Report of the FOCUS Working Group on Surface Water Scenarios, EC Document Reference SANCO/4802/2001- rev.2.

Freeze, R.A. and J. A. Cherry. 1979. Groundwater. Prentice-Hall, Inc., Englewood Cliffs, NJ. 604 pp.

Gerke, H.H. 2006. Preferential flow descriptions for structured soils. Journal of Plant Nutrition and Soil Science, 169, 382 – 400.

Gerke, H.H. & van Genuchten, M.T. 1993. A dual-porosity model for simulating the preferential movement of water and solutes in structured porous media. Water Resources Research, 29, 305 – 319.

Gjettermann, B., Hansen, H.-C.B., Jensen, H.E. & Hansen, S. 2004. Transport of phosphate through artificial macropores during film and pulse flow. Journal of Environmental Quality, 33, 2263–2271.

Green, R.D. and Askew, G.P., 1965. Observations on the biological development of macropores in soils of Romney Marsh. J. Soil Science, 16: 342--349.

Gwo, J.P., Jardine, P.M., Wilson, G.V., Yeh, G.T., 1995. A multiple-pore-region concept to modeling mass transfer in subsurface media. Journal of Hydrology. 164, 217–237.

Haria, A.H., Hodnett, M.G. & Johnson, A.C. 2003. Mechanisms of groundwater recharge and pesticide penetration to a chalk aquifer in southern England. Journal of Hydrology, 275, 122–137.

Heckrath, G., Brookes, P.C., Poulton, P.R. & Goulding, K.W.T. 1995. Phosphorus leaching from soils containing different phosphorus concentrations in the Broadbalk experiment. Journal of Environmental Quality, 24, 904–910.

Hendrickx, J.M.H., Flury, M., 2001. Uniform and preferential flow, mechanisms in the vadose zone, Conceptual Models of Flow and Transport in the Fractured Vadose Zone, National Research Council, National Academy Press, Washington, DC, pp. 149–187.

Hooda, P.S., Moynagh, M., Svoboda, I.F., Edwards, A.C., Anderson, H.A. & Sym, G. 1999. Phosphorus loss in drainflow from intensively managed grassland soils. Journal of Environmental Quality. 28, 1235–1242.

Jarvis, N.J. 1998. Modelling the impact of preferential flow on non-point source pollution. In: Physical Non-Equilibrium in Soils: Modeling and Application (eds H.H. Selim & L. Ma), pp. 195–221. Ann Arbor Press, Chelsea, Michigan.

Jarvis, N.J. 2007. A review of non-equilibrium water flow and solute transport in soil macropores: principles, controlling factors, and consequences for water quality. European Journal of Soil Science. 58, 523–546.

Je´gou, D., Capowiez, Y. & Cluzeau, D. 2001. Interactions between earthworm species in artificial soil cores assessed through the 3D reconstruction of the burrow systems. Geoderma, 102, 123–13

Jørgensen, P.R., McKay, L.D. & Spliid, N.Z.H. 1998. Evaluation of chloride and pesticide transport in a fractured clayey till using large undisturbed columns and numerical modeling. Water Resources Research. 34, 539–553.

Larsson, M.H. & Jarvis, N.J. 2000. Quantifying interactions between compound properties and macropore flow effects on pesticide leaching. Pest Management Science. 56, 133–141.

Lawes, J.B., Gilbert, J.H. & Warington, R.1882. On the Amount and Composition of the Rain and Drainage Waters Collected at Rothamsted. William Clowes & Sons, London.

Lewis, D.T., 1977 Subgroup designation of three Udolls in southeastern Nebraska, Soil Science Society of American Journal. 41, 940-945.

Logsdon, S., McCoy, E.L., Allmaras, R.R., Linden, D.R., 1993. Macropore characterization by indirect methods. Soil Science. 155, 316–324

Luxmoore, R.J., Micao-,1981, meso-and macroporosity of soil, Soil Science Society of American Journal. 45,671.

McDonald, I., 1981. A revised model for the estimation of protein degradability in the rumen. Journal of Agricultural Scienc (Camb.) 96, 251 ±252.

Marshall, T.J. 1959. Relations between water and soil. Tech. comm. 50. Commonwealth Agricultural Bureau, Farnham Royal, UK.

Mori, Y., Iwama, K., Maruyama, T. & Mitsuno, T. 1999a. Discriminating the influence of soil texture and management-induced changes in macropore flow using soft X-rays. Soil Science. 164, 467–482.

Mosely, M.P., 1982. Subsurface flow velocities through selected forest soils, South Island, New Zealand. Journal of Hydrology. 55, 65–92.

Newson, M.D., and Harrison, J.G., 1978. Channe l studies in the Plynlimon experimental catchments. Institute of Hydrology, Wallingford, Oxon. Rep. No. 47, 61pp.

Nelson, W. R., and Baver, L. D. Movement of water through soils in relation to the nature of the pores. Soil Science Society of America. In Proc. 5: 60-76. 1940.

Nutting, P.G., 1930. Physical analysis of oil sands, American Association of Petroleum Geologists Bull. 14, 1337-1349.

Omoti, U. and Wild, A., 1979. Use of fluorescent dyes to mark the pathways of solute movement through soils under leaching conditions, 2. Field experiments. Soil Science. 128: 98-10

Perret, J.S., Prasher, S.O., Kantzas, A. & Langford, C. 1999. Threedimensional quantification of macropore networks in undisturbed soil cores. Soil Science Society of America Journal, 63, 1530–1543.

Pivetz, B.E. & Steenhuis, T.S. 1995. Soil matrix and macropore biodegradation of 2,4-D. Journal of Environmental Quality, 24, 564–570.

Pivetz, B.E., Kelsey, J.W., Steenhuis, T.S. & Alexander, M. 1996. A procedure to calculate biodegradation during preferential flow through heterogeneous soil columns. Soil Science Society of America Journal, 60, 381–388.

Priebe, D.L. & Blackmer, A.M. 1989. Preferential movement of oxygen- 18-labeled water and nitrogen-15-labeled urea through macropores in a Nicollet soil. Journal of Environmental Quality, 18, 66–72.

Pruess, K., Wang, J.S.Y., 1987. Numerical modeling of isothermal and non-isothermal flow in unsaturated fractured rock—a review. In: Evans, D.D., Nicholson, T.J. (Eds.), Flow and Transport through Unsaturated Fractured Rock, Geophysics Monograph, vol. 42. American Geophysical Union, Washington, DC, pp. 11–22.

Ranken, D. W. 1974, Hydrologic properties of soil and subsoil on a steep, forested slope, M.S. thesis, Oregon State University, Corvallis.

Reeves, M.J., 1979, Recharege of the English chalk, A possible meachanism, Engineering Geology, 14(4).

Ritzema HP. 1994. Drainage Principles and Applications. ILRI: The Netherlands.

Roulier, S., Baran, N., Mouvet, C., Stenemo, F., Morvan, X., Albrechtsen, H.-J. et al. 2006. Controls on atrazine leaching through a soilunsaturated fractured limestone sequence at Bre´ villes, France. Journal of Contaminant Hydrology, 84, 81–105.

Russell, E. W. 1973. Soil conditions and plant growth. 10th ed. Longman, London.

Shepherd RG (1989) Correlations of permeability and grain size. Ground Water 27:633–63.

Shipitalo, M.J. & Butt, K.R. 1999. Occupancy and geometrical properties of Lumbricus terrestris L. burrows affecting infiltration. Pedobiologia, 43, 782–794.

Shipitalo, M.J., Dick, W.A., Edwards, W.M., 2000. Conservation tillage and macropore factors that affect water movement and the fate of chemicals. Soil Tillage Research. 53, 167–183.

Šimůnek, J., N.J. Jarvis, M.h . van Genuchten, and A. Gärdenäs. 2003. Review and comparison of models for describing non-equilibrium and preferential flow and transport in the vadose zone. Journal of Hydrology. 272:14–35.

Soil Science Society of America (SSSA). 2002b. Field Water Capacity. Section 3.3.3.2 in SSSA Book Series:5 Methods of Soil Analysis Part 4- Physical Methods, J. H. Dane and C. Topp, eds., Soil Science Society of America, Madison,WI.

Stenemo, F., Jørgensen, P. & Jarvis, N.J. 2005. Linking a one-dimensional pesticide fate model to a three-dimensional groundwater model to simulate pollution risks of shallow and deep groundwater underlying fractured till. Journal of Contaminant Hydrology, 79, 89–106.

Stewart, J.B., Moran, C.J. & Wood, J.T. 1999. Macropore sheath: quantification of plant root and soil macropore association. Plant and Soil, 211, 59–67.

Thomasson, A.J. 1978. Towards an objective classification of soil structure. J. Soil Sci. 29:38–46.

Tippkotter, R. 1983. Morphology spatial arrangement and origin of macropores in some Hapludalfs, West Germany. Geoderma, 29, 355–371.

Todd, D.K. 1959. Groundwater hydrology, Wiley and Sons, New York.

Ule ń, B. & Persson, K. 1999. Field-scale phosphorus losses from a drained clay soil in Sweden. Hydrological Processes, 13, 2801–2812.

White, R.E. 1985a. The influence of macropores on the transport of dissolved and suspended matter through soil. Advances in Soil Science, 3, 95–120.

Wildenschild, D., K.H. Jensen, K. Villholth, and T.H. Illangasekare. 1994. A laboratory analysis of the effect of macropores on solute transport. Ground Water. 32:381–389.

Zaslavsky, D., and G. Kasiff, Theoretical formulation of pipling mechanism in cohesive soils, Geotechnique, 15 (3), 305-316,1965.

.